



Autonomous vehicles: From vehicular control to traffic control

Maria Laura Delle Monache, Jonathan Sprinkle, Ram Vasudevan, Daniel B. Work

► To cite this version:

Maria Laura Delle Monache, Jonathan Sprinkle, Ram Vasudevan, Daniel B. Work. Autonomous vehicles: From vehicular control to traffic control. CDC 2019 - 58th IEEE Conference on Decision and Control, Dec 2019, Nice, France. pp.1-28, 10.1109/CDC40024.2019.9029535 . hal-02335658

HAL Id: hal-02335658

<https://inria.hal.science/hal-02335658>

Submitted on 28 Oct 2019

HAL is a multi-disciplinary open access archive for the deposit and dissemination of scientific research documents, whether they are published or not. The documents may come from teaching and research institutions in France or abroad, or from public or private research centers.

L'archive ouverte pluridisciplinaire **HAL**, est destinée au dépôt et à la diffusion de documents scientifiques de niveau recherche, publiés ou non, émanant des établissements d'enseignement et de recherche français ou étrangers, des laboratoires publics ou privés.

Autonomous vehicles: From vehicular control to traffic control

M. L. Delle Monache*, J. Sprinkle[†], R. Vasudevan [‡], D. Work[§]

Abstract

This article provides an overview of the converging areas of control for autonomous vehicles, and control of the larger transportation system in which a small number of autonomous vehicles serve as actuators of traffic flow. The overview begins by describing the verification techniques and realistic sensor and control interfaces for safe real-time control of autonomous vehicles. Shifting towards a period when autonomous vehicles are present in large numbers, the article reviews classical traffic modeling, estimation, and control techniques, and then considers new methods available to model and use these autonomous vehicles to actuate bulk traffic flow composed primarily of human-piloted vehicles.

1 Introduction

This overview considers the converging areas of control for autonomous vehicles (AVs) and control of traffic with AVs. The overview starts on the vehicle and addresses core challenges in which safety and real-time constraints must both be met when solving vehicular control problems. Highlighting this issue further, we then proceed to explore the challenges of controlling real vehicles with current off-the-shelf vehicle interfaces, and how they may be overcome. Examples from a real AV platform with datasets and simulation environments will be introduced. We then expand the context by considering the problems of traffic estimation and control which are evolving due to the introduction of AVs in the flow. We first provide the theoretical underpinnings with an overview of the relevant partial differential equation (PDE) and ordinary differential equation (ODE) models used to describe traffic, and then provide an overview of the estimation and control problems that arise from these models. A brief summary of the overview is provided here in the introduction.

1.1 Techniques for online verification of AV control

Autonomous vehicles operate with limited sensor horizons in unpredictable environments. To do so, they use a receding-horizon strategy to plan trajectories by executing a short plan while creating the next plan. To ensure that these trajectories can be executed safely, a variety of techniques have been proposed for verification. These verification techniques (described in Section 2) can be broadly divided into three categories according to how they ensure safety at run-time.

The first category of techniques, which we refer to as *check methods*, focus on just verifying the safe operation of a pre-computed reference trajectory by performing reachability analysis at run-time [2, 3, 87, 88]. In practice, these techniques can be applied to determine which of a finite family of pre-computed reference trajectories are safe. After performing verification on the finite family of trajectories, one can choose amongst those verified to behave safely the reference trajectory that best achieves a desired goal.

The second category of approaches, which we refer to as *correct methods*, modify a control input that is generated by an optimization program to ensure that an autonomous system will behave in a safe manner [45, 61, 124]. The optimization problem in this instance encodes achieving some user desired objective, but the verified

*M. L. Delle Monache is with the NeCS team at the Univ. Grenoble Alpes, Inria, CNRS, Grenoble INP, GIPSA-Lab, 38000 Grenoble, France. m.l.dellemonache@inria.fr.

[†]J. Sprinkle is with the Dept. of Electrical and Computer Engineering, University of Arizona, Tucson, AZ. sprinkle@ece.arizona.edu.

[‡]R. Vasudevan is with the Dept. of Mechanical Engineering, University of Michigan, Ann Arbor, MI. ramv@umich.edu.

[§]D. Work is with the Dept. of Civil & Environmental Engineering, Vanderbilt University, Nashville, TN. dan.work@vanderbilt.edu.

performance of the controller is ensured by correcting a generated control input after optimization has occurred. Though powerful, these methods to date have been applied primarily to control of unmanned aerial vehicles.

The final category of approaches, which we refer to as *select methods*, instead optimize directly over a set of trajectories that are verified at run-time to behave safely [20, 75, 86, 102, 150]. This is accomplished by introducing a constraint into the optimization program that enforces safety of the synthesized controller. Section 2 provides an overview on check and select methods since these have been directly applied to ground vehicle control.

1.2 Realistic control and sensing for AVs

In Section 3, we bridge the advanced verification problems discussed in Section 2, to address realistic challenges with following a time-varying trajectory with respect to control and sensing for connected autonomous vehicles. The approach is to discuss how to go beyond following the trajectory from Point A to Point B, to discuss margins of error, and timeliness with regards to the realistic errors of sensors. Solutions to challenge problems will demonstrate case studies for how to follow time-varying velocity trajectories [14] while considering the comfort of passengers, as well as why low-level controllers may require modification.

1.3 Traffic modeling

Section 4 provides an overview of the mathematics of traffic flow modeling via dynamical systems at different levels of abstraction (discrete, continuous), and how to use these models for traffic management applications. We will present the most common dynamical models used in traffic flow and give some insight about their analytical and numerical properties. The following class of models will be described:

- Microscopic models: we will look at the most common microscopic models as the follow-the-leader [17], optimal velocity models [9] and Intelligent Driver Model [72]. These models are usually described as systems of ODEs for N vehicles:

$$\begin{cases} \dot{x}_i = v_i & i = 1, \dots, N \\ \dot{x}_i = a(x_i, v_i, x_{i+1}, v_{i+1}) & i = 1, \dots, N \end{cases}$$

with (x_i, v_i) being the position and the speed of vehicle i , respectively, and $a(\cdot)$ is an acceleration function.

- Macroscopic models: we will look at first-order models like LWR [85, 115]. These models are written as PDEs describing conservation of mass (with higher order models also considering momentum). The most common model is the LWR, which is the building block of all the others, is written as:

$$\partial_t \rho + \partial_x f(\rho) = 0$$

where ρ is the traffic density and $f(\rho)$ is a flux function.

- Mixed micro-macro models: Lastly, mixed models will be discussed. We will look at how to include both scales in a single model to represent traffic at a average scale but with influence from phenomena that happen at a microscopic scale. These models are PDE-ODE models [36, 78] where the PDE will describe the overall traffic dynamics while the ODE will capture a particular dynamics, for example, of an autonomous vehicle.

1.4 Eulerian to Lagrangian traffic estimation & control

This overview leverages the described traffic flow models to overview the classical approaches for highway traffic estimation (e.g., Kalman based filters [51, 120] and particle filters [93]) and traffic control (e.g., ramp metering and variable speed limits [42]) based on sensors and actuators that are fixed in place.

Recognizing the role of Lagrangian (or mobile) sensing that completely transforms the traffic estimation landscape, we explore emerging methods for traffic control in which AVs serve as actuators to stabilize traffic flow [125]. Like low penetration rate Lagrangian sensing, which can achieve very accurate traffic state estimates, it is now possible to use automated vehicles at low penetration rates for traffic control. We summarize major field experiments in traffic estimation and control, including recent results where AV platforms using realistic sensing and control interfaces are modeled and controlled to eliminate human-generated phantom traffic jams that seemingly occur without cause but are in fact a result of string-unstable car following dynamics [125].

2 Techniques for online verification of AV control

This section provides an overview on check and select methods since these have been directly applied to ground vehicle control. To formulate these pair of techniques, we begin with defining a vehicle model and describing the environment in which the vehicle is operating. After describing how check and select methods formulate the online verification task, this section concludes with a brief description on how these techniques have been applied to autonomous vehicles.

2.1 Preliminaries

The verification task requires formulating the vehicle dynamics and describing environmental constraints that must be respected during operation. Suppose the vehicle's dynamics are defined using a *high-fidelity model* $f_{hi} : T \times X_{hi} \times U \rightarrow \mathbb{R}^{n_{hi}}$ for which

$$\dot{x}_{hi}(t) = f_{hi}(x_{hi}(t), u(t)), \quad (1)$$

where time t is in the *planning time horizon* $T = [t_0, t_f]$. The state x_{hi} is in the space $X_{hi} \subset \mathbb{R}^{n_{hi}}$, and inputs are drawn from $U \subset \mathbb{R}^{n_U}$. Since planning is done in a receding-horizon fashion, without loss of generality, let each planned trajectory (i.e., each planning iteration) begin at $t_0 = 0$.

Since autonomous vehicles operate on the ground, we make the following assumption:

Assumption 1. *The autonomous vehicle operates in the plane. Define $X \subset \mathbb{R}^2$ as the spatial coordinates of the vehicle's body such that X corresponds to the first two dimensions of X_{hi} . The operator $\text{proj}_X : X_{hi} \rightarrow X$ projects points in X_{hi} to X via the identity relation. The vehicle is a rigid body whose footprint (i.e., body) lies in the compact, convex set $X_0 \subset X$ at $t = 0$.*

The autonomous vehicle operates in an environment where it is surrounded by other road users. We describe these other road users using the following definition:

Definition 2. *At any time $t \geq 0$, an obstacle is a subset of X that the vehicle should not have non-empty intersection with. Denote the n^{th} obstacle at t by $O_t^n \subset X$ for each $n \in \{1, \dots, N_{\text{obs}}\}$.*

During operation, the autonomous vehicle is typically tasked with reaching some user-specified location in X without colliding with any obstacles. To ensure safe operation in environments that may be unknown before operation, one must be able to verify in real-time that the controller generates a trajectory for the autonomous vehicle which avoids collisions with obstacles. Tackling this problem is challenging due to the size of the state space of the vehicle dynamic model and its non-linearity.

2.2 Check Methods

Rather than focusing on constructing an arbitrary controller, check methods verify the safe operation of a given reference input $u_{\text{ref}} : T \rightarrow U$ beginning from an initial set of states $X_{hi,0} \subset X_{hi}$. In particular, note that for each $x_{hi,0}$ in $X_{hi,0}$, $\text{proj}_X(x_{hi,0})$ is in X_0 . To account for this set of initial conditions, one can construct the forward reachable set of the vehicle under this reference input:

$$\begin{aligned} F_{\text{check}}(X_{hi,0}, u_{\text{ref}}) = & \{(t, x) \in T \times X \mid \exists x_{hi,0} \in X_{hi,0} \text{ s.t.} \\ & \dot{x}_{hi}(\tau) = f_{hi}(x_{hi}(\tau), u_{\text{ref}}(\tau)), \forall \tau \in T, \\ & x_{hi}(0) = x_{hi,0}, \text{ and } x_{hi}(t) = x\}. \end{aligned} \quad (2)$$

If this set can be constructed at run-time and represented in a computationally amenable fashion, then it can be intersected with obstacles to identify whether a reference input can be applied in a safe manner. Note, though we do not describe it here, this approach can be extended to account for model and sensor uncertainty in the vehicle model.

Since computing the set of reachable states exactly is challenging, check methods focus on constructing an outer approximation to the reachable set. To compute this over approximation, check methods typically discretize time and construct the reachable set about a pre-computed reference trajectory. Since reachable sets can be computed rapidly for linear systems, certain check methods linearize the vehicle dynamics in a conservative fashion. That is, all possible linearization errors are considered to generate an outer approximation of the reachable set

which is represented as a zonotope [3, 4]. If the intersection of this zonotope description of the reachable set with all obstacles is empty, then the specific reference trajectory is verified to behave safely.

On the other hand, one can construct the reachable set in an off-line fashion by applying sums-of-squares optimization techniques [88]. These formulations reduce the computation of the reachable set to a semidefinite program whose solution generates a polynomial whose 0-superlevel set coincides with the reachable set of the system. If the intersection of the 0-superlevel set of this polynomial with all obstacles is empty, then the specific reference trajectory is verified to behave safely. Since these semidefinite programming based techniques perform off-line computation of the reachable set of a family of reference trajectories, they also introduce a notion of sequential compositability that describes when the states at the final time of one reachable set belongs to the initial states of another reachable set.

Finally, to ensure that a safe reference trajectory can always be found at run-time, check methods typically append a fail-safe maneuver to each trajectory. This fail-safe maneuver, which is typically a braking maneuver, always brings the vehicle to a complete stop and can at least guarantee that any trajectory that is applied will ensure that the vehicle will not purposefully run into other obstacles. However, this is unable to guarantee that the vehicle will not be run into by other surrounding vehicles.

2.3 Select Methods

In contrast to check methods, which rely upon selecting amongst a finite number of trajectories, select methods typically select amongst a continuum of possible trajectories by solving an optimization problem. To guarantee the safe behavior of the computed trajectory, select methods introduce an additional constraint. The formulation of this constraint is distinct for each type of select method. In the instance of control barrier functions, for example, this constraint, at each instance in time, can usually be represented as a linear constraint, and the optimization problem can be formulated as a convex quadratic program [5]. However, this only allows one to perform control design at a single time step rather than over a time horizon. This can lead to conservative behavior. To simplify exposition and since a tutorial on control barrier functions has published recently [5], this subsection focuses on a different, recently developed select technique entitled Reachability-based Trajectory Design (RTD) [75, 138, 139].

To ensure that a safe trajectory can always be found by the optimization algorithm, RTD begins by making the following assumption:

Assumption 3. *During each planning iteration, the vehicle has $\tau_{\text{plan}} > 0$ amount of time to pick a new input. If the autonomous vehicle cannot find a new input in a planning iteration, it begins a “fail-safe” maneuver. In this work, the fail-safe maneuver is braking to a stop; then the autonomous vehicle stays stopped until a new input is found.*

Since planning with the high-fidelity model can be computationally prohibitive, RTD utilizes a simplified model called a trajectory-producing model:

Definition 4. *Let $T = T_{\text{move}} \cup T_{\text{brake}}(k) \cup T_{\text{stop}}(k)$. We call $T_{\text{move}} := [0, \tau_{\text{plan}}]$ the moving phase; $T_{\text{brake}}(k) := [\tau_{\text{plan}}, \tau_{\text{plan}} + \tau_{\text{brake}}(k)]$ the braking phase, and $T_{\text{stop}}(k) := [\tau_{\text{plan}} + \tau_{\text{brake}}(k), t_f]$ the stopped phase. The function $\tau_{\text{brake}} : K \rightarrow \mathbb{R}_{\geq 0}$ is the braking time of each desired trajectory. The trajectory-producing model $f : T \times X \times K \rightarrow \mathbb{R}^2$ is then:*

$$\dot{x}(t) = f(t, x, k) = \begin{cases} f_{\text{move}}(t, x, k), & t \in T_{\text{plan}} \\ f_{\text{brake}}(t, x, k), & t \in T_{\text{brake}} \\ f_{\text{stop}}(t, x, k), & t \in T_{\text{stop}} \end{cases} \quad (3)$$

The trajectory producing model generates *desired trajectories* in X . The space $K \subset \mathbb{R}^{n_K}$ contains *trajectory parameters* which parameterize the desired trajectories.

Given a desired trajectory parameterized by $k \in K$, the autonomous vehicle uses a low-level controller $u_k : T \times X_{\text{hi}} \times K \rightarrow U$ to track it. Note that u_k can be any feedback controller, but typically cannot perfectly track desired trajectories. We say that the autonomous vehicle “tracks k ” to mean that it tracks a desired trajectory parameterized by k . To simplify exposition, we do not show dependence on k for T_{brake} and T_{stop} hereafter. Note that $f_{\text{stop}}(t, x, k) = 0$ usually; we write f_{stop} to illustrate that coming to a stop (i.e., completing the fail-safe maneuver) is part of every desired trajectory.

To bound the spatial difference between the autonomous vehicle and the desired trajectory at any time, RTD defines a *tracking error*:

Assumption 5. Let $i \in \{\text{move, brake, stop}\}$ index the phases of T and let $j \in \{1, 2\}$ index the first and second dimension in X , respectively. Then, for each phase and state pair (i, j) , there exists a function $g_{i,j} : T \times K \rightarrow \mathbb{R}_{\geq 0}$ such that $\text{supp}(g_{i,j}) \subseteq T_i \times K$ and for any $t \in T$ and $k \in K$ the following inequality holds:

$$\max_{x_{hi,0} \in X_{hi,0}} |x_{hi,j}(t; x_{hi,0}, k) - x_j(t; x_0, k)| \leq \int_0^t \max_i \{g_{i,j}(\tau, k)\} d\tau, \quad (4)$$

where $X_{hi,0} = \{x_{hi} \in X_{hi} \mid \text{proj}_X(x_{hi}) \in X_0\}$, $x_{hi,j}(t; x_{hi,0}, k)$ is the solution to (1) in state j at time t beginning from $x_{hi,0}$ under a control input u_k , and $x_j(t; x_0, k)$ is the solution to (3) in state j at time t beginning from $x(0) = \text{proj}_X(x_{hi,0})$ under a trajectory parameter k .

RTD combines these $g_{i,j}$ to create the tracking error function $g : T \times K \rightarrow (\mathbb{R}_{\geq 0})^2$, written as $g = (g_1, g_2)$, such that $g_j(t, k) = \max_i \{g_{i,j}(t, k)\}$. The tracking error function lets RTD “match” the spatial component of the high-fidelity model’s trajectories using the trajectory-producing model.

Lemma 6. [75, Lemma 12] For each $x_{hi,0} \in \{x_{hi} \in X_{hi} \mid \text{proj}_X(x_{hi}) \in X_0\}$ and $k \in K$, there exists a $d \in L_d(T)$ such that $\text{proj}_X(x_{hi}(t; x_{hi,0}, k)) = \text{proj}_X(x_{hi,0}) + \int_0^t (f(\tau, x(\tau; \text{proj}_X(x_{hi,0}), k), k) + g(\tau, k)d(\tau)) d\tau$ for each $t \in T$, where $x_{hi}(t; x_{hi,0}, k)$ is the solution to (1) at time t beginning from $x_{hi,0}$ under a control input u_k and $x(t; \text{proj}_X(x_{hi,0}), k)$ is the solution to (3) at time t beginning from $\text{proj}_X(x_{hi,0})$ under a trajectory parameter k .

At each planning iteration, RTD selects a desired trajectory that the robot can track while not-at-fault. To understand how this is done, for a set A let $\mathcal{P}(A)$ denote the power set of A . RTD attempts to compute a *not-at-fault map* $\varphi : \mathcal{P}(T \times X) \rightarrow \mathcal{P}(K)$ from time and space (where obstacles live) to the trajectory parameters that, when tracked, guarantee the autonomous vehicle is not-at-fault. Computing such a map requires understanding where the autonomous vehicle could be at any time while tracking any desired trajectory. To construct this map, RTD computes the forward reachable set of the system.

The forward reachable set contains all times and states reachable by the autonomous vehicle, described by (1), when tracking any trajectory produced by (3). By Lemma 6, the trajectory-producing model and tracking error function can “match” any high-fidelity model trajectory on the space $T \times X$. Define the forward reachable set of the trajectory producing model plus tracking error as

$$\begin{aligned} F = & \{(t, x) \in T \times X \mid \exists (x_0, k) \in X_0 \times K, d \in L_d(T) \text{ s.t.} \\ & \dot{x}(\tau) = f(\tau, \tilde{x}(\tau), k) + g(\tau, k) \circ d(\tau) \forall \tau \in T, \\ & \tilde{x}(0) = x_0, \text{ and } \tilde{x}(t) = x\}. \end{aligned} \quad (5)$$

Per (3), the dynamics f and tracking error g are time-switched with three phases. As described earlier, exactly computing the forward reachable set can be computationally challenging. RTD therefore computes an outer approximation of the forward reachable set with three semidefinite programs, one for each phase. The result of each semidefinite programs is a polynomial function $w_i \in C(T \times X \times K)$ whose 1-superlevel set is an outer approximation to the forward reachable set in each phase of the dynamics [138, Lemma 16].

We next describe how RTD conservatively approximates the not-at-fault map φ . Extend the domain of each w_i to $T \times X \times K$ by setting $w_i(t, \cdot, \cdot) = 0 \forall t \notin T_i$. Then, combine the w_i into a single $w : T \times X \times K \rightarrow \mathbb{R}$ as $w(t, x, k) = \max_i \{w_i(t, x, k)\}$. Since the 1-superlevel set of each w_i is an outer approximation to the forward reachable set, $w(t, x, k) \geq 1$ on trajectories of the high-fidelity model. Now define $\tilde{\varphi} : \mathcal{P}(T \times X) \rightarrow \mathcal{P}(K)$ as

$$\tilde{\varphi}(T' \times X') = \{k \in K \mid w(t, x, k) < 1, t \in T', x \in X'\}. \quad (6)$$

Since w outer approximates the forward reachable set, $\tilde{\varphi}$ under approximates φ (meaning $k \in \tilde{\varphi}(t, x) \implies k \in \varphi(t, x)$).

During online motion planning, one can require that the trajectory parameters be chosen from $k \in \tilde{\varphi}(O_i^n)$ for all $t \in T$ and $n \in \{1, \dots, N_{\text{obs}}\}$ to ensure that any designed trajectory is verified to behave safely. However, $\tilde{\varphi}$ may not be a convex function and verified online motion planning may require solving a nonlinear optimization program. Nevertheless, due to the formulation of the fail-safe maneuver, one can always prove that the vehicle will behave safely when applying RTD in a static environment [75].

2.4 Applications of Check and Select Methods

These techniques for online verification have been applied across a variety of different vehicle platforms while performing various tasks. For instance, a zonotope-based, check method has been applied to verify the safety of

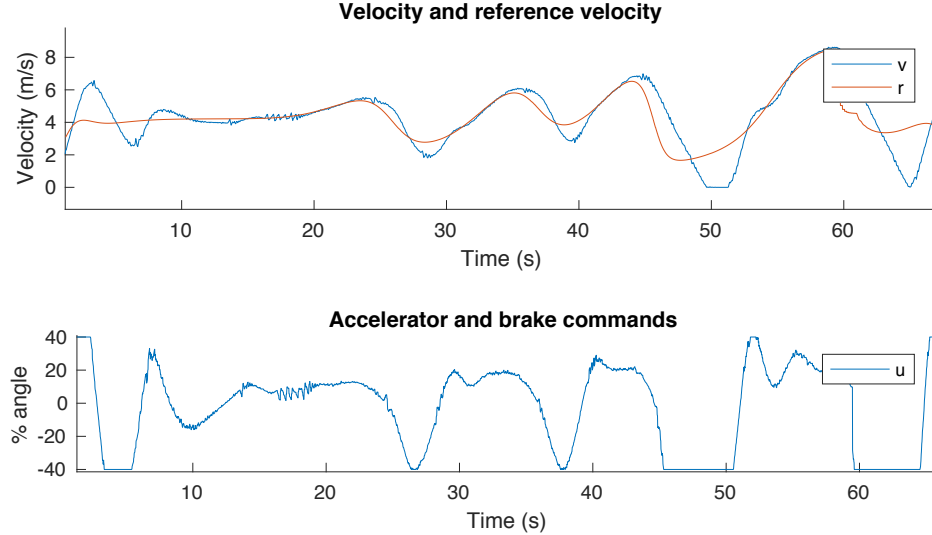


Figure 1: Use of a traditional cruise controller to follow a time-varying trajectory. The accelerator is in use when the angle is greater than 0, and the brake is in use when the angle is less than 0. These values are plotted as percentages of the maximum value.

lane change maneuvers on a Cadillac SRX at *Robot City* in Pittsburgh [3]. This verification procedure ensured that a lane change avoided any collisions with traffic participants while ensuring that the vehicle remained within pre-specified road boundaries. On the other hand, control barrier function-based, select methods have been applied to verify the safety of adaptive cruise control and lane keeping systems [6, 102, 150]. In these instances, the quadratic-programming based formulation can even be implemented without online optimization, since the solution is known in closed form. RTD has been applied to verify the safe operation of an autonomous vehicle required to perform arbitrary motion in a static environment [139]. RTD has also been applied to verify the operation of an autonomous vehicle operating in dynamic environments [138]; however, due to the potential existence of malicious road actors, all that can be guaranteed is that the autonomous vehicle being controlled using RTD will never be traveling with non-zero speed and collide with other road users.

3 Realistic control & sensing for AVs

In the previous section, trajectories for the vehicle to follow were defined using coordinates of $X \subset \mathbb{R}^2$, with obstacles and trajectories defined as time-varying $(t, x) \in T \times X$, or to express as a time varying signal, a desired trajectory $x(t)$. Differentiating this curve and projecting along the direction of travel would provide a straightforward reference velocity $r(t)$ which could be provided to the vehicle to follow. Beyond the trajectory generator in the previous section, other kinds of reference velocities could be imagined which—although smooth—could be difficult to follow without a horizon upon which to predict and optimize the controller.

Accumulated error for a velocity-following controller could be tolerated when going slower than desired, but if the reference trajectory is used to avoid a collision, then a fast reaction must be used. The use of the vehicle's brake to decelerate, however, could pose a challenge to any following vehicles if it results in erratic behavior, or if the brake light indicators flash in a way not typically observed by human drivers when following a vehicle under human control.

Examples of this behavior with a traditional cruise-controller designed to maintain steady-state velocity input are found in Figure 1. Although the reference trajectory r does not fall below 0 m/s, the vehicle comes to a stop near the time 50 s due to overshoot when braking. Similarly, significant delay is observed when the reference velocity is reduced near 25, 35, and 45 s, indicating challenges if the reference trajectory is intended to avoid collision with a leading vehicle.

The problem thus has competing requirements of rapid deceleration (only with significant error in the reference input) and rapid acceleration (only if the brake is not depressed). This motivates a switched controller design. The switches between the system modes are derived directly from the conditions:

1. Large reference velocity error, necessitating braking

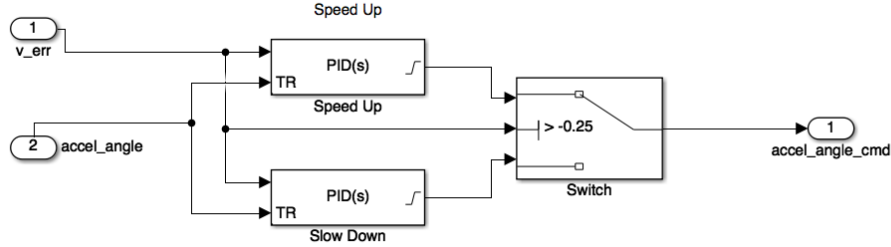


Figure 2: A two-mode switched controller permits faster reaction to slow down, if the reference error is significant.

2. Large reference velocity error, necessitating acceleration
3. Maintain steady-state velocity input
4. Synthesize local reference velocity to reduce overshoot

Thus, a multi-state switched system is proposed. In each state, a reference model is used to tune PID control to achieve the ramp and step inputs. Switches between modes are taken when state error exceeds the braking (or acceleration) thresholds that are commonly observed in human driving [14].

3.1 System identification

The expected range of use for the controller is $0 \leq v \leq 10 \text{ m/s}$. In order to tune the controller in this range, an open loop input $0 \leq u_1(t) \leq 1$ is used, which represents the minimum to maximum commanded accelerator angle.

The approach to system ID uses reference inputs ranging from $u_1 \in \{0.2, 0.3, 0.4\}$ to develop the following first-order model for velocity based on $u_1 > 0$:

$$G(s) = \frac{0.1333}{s + 0.5} \quad (7)$$

This linear approximation is deemed suitable based on reasonable approximations at commands u_1 of 0.3 and 0.4 producing approximately the same response after adjusting input gain magnitude. To overcome differences in actuation between brake and accelerator, we design the controller model for slowing down to have higher gain in order to account for a model mismatch.

3.2 Model description

The model has two discrete modes, the first to speed up, and the second to slow down (Figure 2). The reason for these two modes is to enable faster tracking of the reference velocity if braking is required. The brake is applied only with error of -0.25 m/s or larger in magnitude. This permits a commanded accelerator angle of 0 for small braking commands, thus depending on the idle speed of the vehicle to slow the car.

Each model has a PID controller with an anti-windup configuration. The PID settings are intended for each to produce sufficiently fast results with little overshoot. The parameters for the speedup controller are 1.9s rise time, with less than 10% overshoot and no steady state error. For the slowdown controller, the rise time is 0.5s with approximately 10% overshoot.

3.3 Analysis

The relatively small amount of overshoot for the speedup controller prevents hysteresis between the two modes during acceleration. Up to a step input of 4 m/s the overshoot will result in less than -0.25 m/s of error, which would not switch to the braking controller. When accelerating from rest, the controller is best served by a supervisory controller that ramps up the reference controller to avoid a significant step input error.

To validate the design with realistic simulation models, we use the system model given in (7) as the plant, and provide a time-varying reference velocity. We utilize a transport delay to approximate the application of actuators

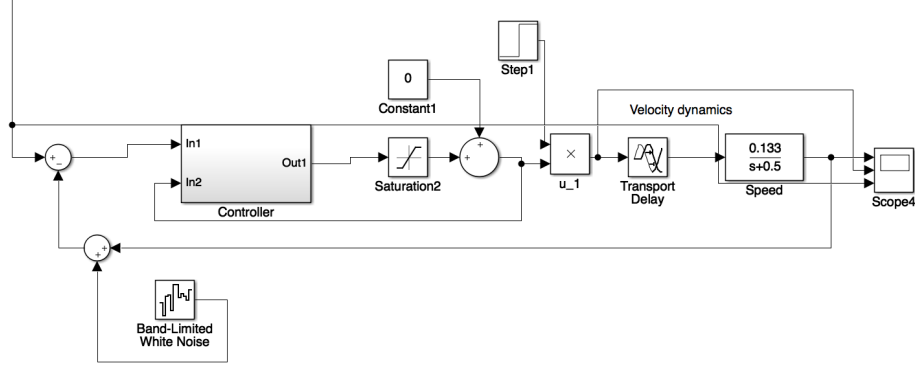


Figure 3: Simulation of the open-loop transfer function under control by the switched system. The reference velocity is passed in from the parent model.

and the discrete-event message passing utilized for the vehicle control computer, running at 20 Hz. In Figure 3 the assumption of communication delay, as well as noise in the estimation of velocity, are shown as realistic disturbances that the controller should reject.

Figure 4 demonstrates rejection of both sensor noise and delay, as well as avoidance of windup due to inactivity in the plant model if the controller is not active even though reference inputs are being received.

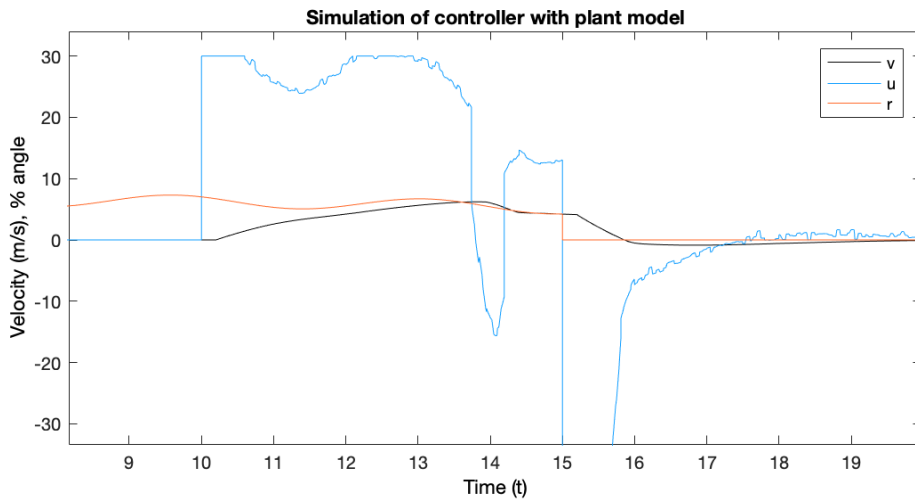


Figure 4: The simulated system's tracking response to a realistic curve.

The designed system is performing sufficiently well against the plant model used in design, with additive noise and transport delay, while also avoiding windup that can cause challenges when waiting to execute a command. The next step is transition to hardware-in-the-loop testing for physical platform validation.

3.4 Physical platform validation

The motivation of the redesign of this controller highlighted in Figure 1 featured specific input reference velocities, and the design section provided some reference velocity trajectories that seemed to behave sufficiently well. We now take these trajectories and provide them to the updated controller, but with the physical platform in the loop, rather than the simulated platform.

In Figure 5 the results of hardware-in-the-loop validation are presented. In order to produce these results, the same time-varying velocity was provided as was utilized when motivating the work. In the updated controller, the previously noted overshoot when braking and accelerating are each tempered, and the delay when following the trajectory is reduced.

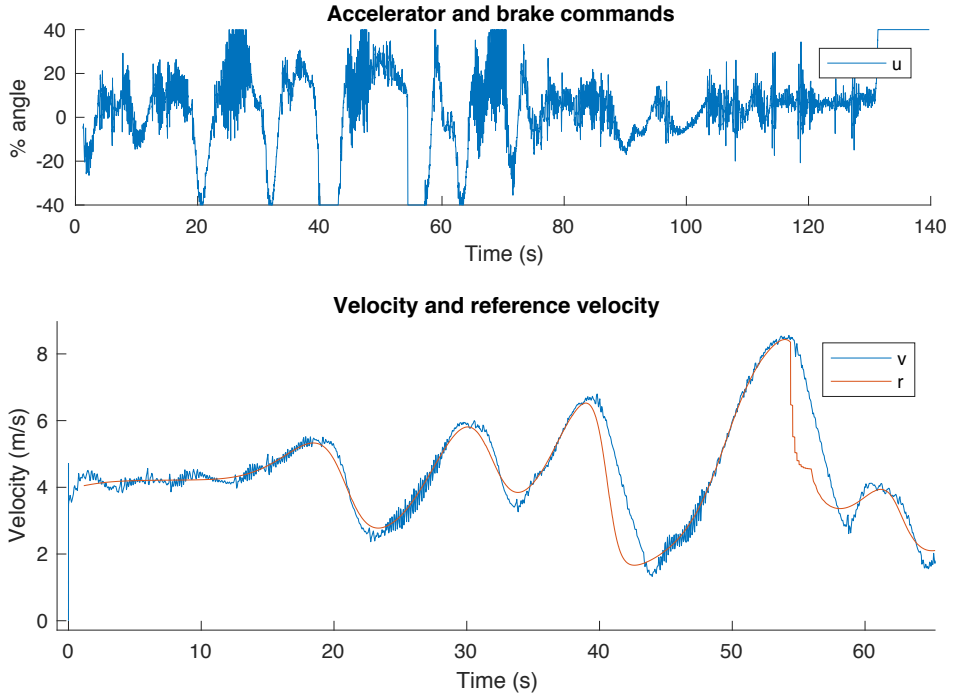


Figure 5: Results of time-varying trajectory following with the updated controller from Figure 2.

With respect to the overall process for design and implementation, the approach of using model-based design and regression testing is one which lends itself to the validation of the controllers as they are redesigned. By capturing the outputs of optimization tools that are planning to utilize the car, we are capturing the desired velocity *inputs* to the vehicle (these become $r(t)$). An initial hardware exploration of executing those $r(t)$ control inputs resulted in a determination that the performance was likely to do more harm than good, when it came to controlling traffic. Having those inputs as a regression test permitted execution of the desired inputs in order to tune the controller, simulate its performance with a stand-in model, compare that model's performance with the system-identified model, and finally check the overall performance with hardware-in-the-loop execution of the updated controller—which was deployed onto the vehicle through code-generation. Without capturing the desired inputs (and outputs) as part of the process, it was not possible to compare the original designs to the final ones, and the use of the model-based approach permitted direct specification of the controller in MATLAB/Simulink, which could be then generated as C/C++ code using code generation and middleware such as that of the Robotic System Toolbox.

3.5 Discussion

In this section we have demonstrated the ability to track a reference velocity trajectory with reasonable accuracy, little overshoot, and acceptable delay. It is worth briefly discussing why we would want to follow a reference velocity trajectory, in addition to a trajectory in X .

Within the context of vehicle control for safety, it is important to understand the fundamental limitations of the platform in terms of maximum braking and the delay of accelerator, brake and other actuators. When coupled with sensor data of the surrounding environment, and the computation time required to evaluate the state of the system and calculate a new control input, the constraints around the system and its performance are clearly formidable. For example, while the results in Figure 5 demonstrate that although the updated controller does not result in the vehicle coming to a stop, there are other limitations clearly evident. For example, the vehicle is unable to slow down as quickly as the reference trajectory—thus, there are maximum decelerations (and likewise, accelerations) that depend on the physical dynamics of the system. These should be taken into account when designing the velocity trajectories, as understanding them will improve the overall safety of the system.

Importantly, the time-varying velocity trajectories tie closely with the concept of using vehicles to control the flow of traffic behind them. This goal can be achieved *only* if the vehicle can follow these trajectories suffi-

ciently closely. If there is consistent error when following the trajectories, then the effect may be to amplify the disturbances, rather than dampen them.

4 Traffic modeling

4.1 Introduction

In this section, we will consider what happens at a traffic level, expanding from the dynamics and control of the single vehicle to the dynamics of traffic as a whole. In particular, we will start from classical approaches to traffic modeling to move later on modeling approaches that includes new technologies and in particular we will see how to track and include the dynamics of a single vehicle, which can be autonomous, among the rest of the traffic. We will first show how traffic can be modeled using different methods and then we see how these methods can be unified in an unique approach to have a complete traffic dynamics which includes humans and automated vehicles.

Traffic is a phenomenon that is complex and hard to simulate and model due to the presence of traffic jams. Several approaches have been developed during the years, each one focusing on some particular traffic characteristic. The main purposes for traffic modeling is for example, minimization of congestion, accidents, pollution and safety issues. There are several ways of modeling traffic flow and the different methods can be grouped in three big categories: microscopic models, macroscopic models and mixed micro-macro models. Microscopic models describe the trajectory of each single car in the road with an ordinary differential equation. The basic models are the car-following ones. The main assumption of the car-following models is that an individual car's motion only depends on the car ahead; see [9, 17, 19, 118]. Macroscopic models, instead, consider traffic as a fluid. The first ones to introduce this concept were Lighthill, Whitham [85] and, independently, Richards [115], in the fifties. They were the first ones to describe traffic flow with equations coming from fluid dynamics, using a non linear hyperbolic partial differential equation. More recently, several authors proposed models on networks that take into account different types of solutions at the intersections, see [21, 22, 38, 46–49, 64, 65, 89] and references therein. In all these works, the road network is described as a graph, incoming and outgoing roads are the edges while the junctions are described by the nodes. More recently, several authors have been investigating different areas of study in order to include more features in the models. In particular, some models were proposed that track a single vehicle moving in traffic. In these models, the single vehicle trajectory is described with an ODE generating coupled PDE-ODE models to take into account the advantages of a microscopic approach and a macroscopic one.

4.2 Microscopic models

Microscopic models are based on ordinary differential equations describing the dynamics of each single vehicle. The most used mathematical formulation is the one of car-following models. They represent the traffic dynamics from the perspectives of each single couple driver-car. The first car-following models were proposed in the 1950's in [108, 113, 114]. The general form of microscopic models for N vehicles on a road is as follows:

$$\begin{cases} \dot{x}_i = v_i & i = 1, \dots, N \\ \dot{v}_i = a_i(v_i, \Delta v_i, \Delta x_i) & i = 1, \dots, N \end{cases} \quad (8)$$

In (8), x_i is the position of each single vehicle, v_i is its speed, and $\Delta x_i = x_{i+1} - x_i$ represents the headway between two consecutive vehicles and $\Delta v_i = v_{i+1} - v_i$ its relative speed. The term a_i indicates an acceleration function. The two most common microscopic car-following models are the follow-the-leader model [109, 113, 114] and the optimal velocity model [9].

4.2.1 Follow-the-leader model

This model was introduced in [109, 113, 114] and it assumes that the acceleration of a vehicle depends on the neighboring vehicles. The main influence comes from the vehicle in front, whose index is $i + 1$, that is also called leading vehicle. This model is described by:

$$\begin{cases} \dot{x}_i = v_i \\ \dot{v}_i = C \frac{v_{i+1} - v_i}{x_{i+1} - x_i} \end{cases} \quad 1 \leq i \leq N \quad , \quad (9)$$

where C is a constant with appropriate dimension. This model has the following properties:

- The acceleration depends on the relative velocity $\Delta v = v_{i+1} - v_i$;
- The velocity $v_i(t)$ of the vehicle depends on the velocity of the vehicle in front such that the distance from the vehicle in front is safe.

4.2.2 Optimal velocity model

The optimal velocity model was introduced by [9]. It is a microscopic model where the acceleration function is given by

$$a_i = (V_{\text{opt}}(\Delta x_i) - v_i).$$

V_{opt} is called the optimal velocity function and it indicates the optimal speed at which each driver would like to go based on their distance Δx_i to the car in front. The optimal velocity term as introduced by Bando et al, in [9] has the following form:

$$V_{\text{opt}} = V_{\max} \frac{\tanh\left(\frac{\Delta x_i}{d_0} - 2\right) + \tanh 2}{1 + \tanh 2} \quad (10)$$

with the desired speed V_{\max} and the desired headway d_0 .

4.3 Macroscopic models

Macroscopic models are based on hyperbolic conservation laws that are nonlinear partial differential equations where the unknown variable is a conserved quantity. A scalar conservation law in one space dimension is a first order partial differential equation of the form

$$\partial_t \rho + \partial_x f(\rho) = 0 \quad (x, t) \in \mathbb{R} \times \mathbb{R}^+$$

where ρ is the conserved quantity and f is the flux function.

4.3.1 LWR model

In the fifties Lighthill and Whitham [85] and, independently Richards [115] introduced a hydrodynamic model for traffic flow on a single infinite road. They were the first to describe traffic as a fluid and used the equations from fluid-dynamics to describe its behavior. Their model is based on the conservation of cars and it consists of a single conservation law, which describe the evolution of the traffic in time in terms of macroscopic variables (density, average speed of cars).

Let us now see how this model is developed. Let us consider a unidirectional stretch of road which is modeled by an interval $I = [a, b]$ with $a < b$, $a, b \in \mathbb{R}$ and the possibility of either a and b equal to ∞ . The model is based on the equation for the conservation of mass.

$$\partial_t \rho + \partial_x f(\rho) = 0, \quad (t, x) \in \mathbb{R}^+ \times \mathbb{R} \quad (11)$$

where $\rho = \rho(t, x) \in [0, \rho_{\max}]$ is the density (number of cars per unit length), ρ_{\max} being the maximal density allowed in the car. The flow $f : [0, \rho_{\max}] \rightarrow \mathbb{R}$ is a smooth flux function that is usually given by $f(\rho) = \rho v$ where $v = v(\rho)$ is the average speed of cars.

This model is known in the traffic literature as LWR model. The main assumption for the LWR model is that the velocity depends only on the density of cars. A reasonable supposition is that v is a decreasing function of the density.

In the transportation literature, the graph that links the flux and the density is called fundamental diagram. According to the choice of the velocity function we can have a variety of fundamental diagrams. The simplest choice is a linear function of the density,

$$v(\rho) = v_{\max} \left(1 - \frac{\rho}{\rho_{\max}}\right), \quad (12)$$

see Figure 6. The corresponding fundamental diagram is obtained by multiplying the density by the speed. This gives a C^2 concave function like the one in Figure 7. This flow-density relation was introduced by Greenshields [55] and it is one of the most widely used in the mathematics community, with a triangular shaped diagram being another popular choice.

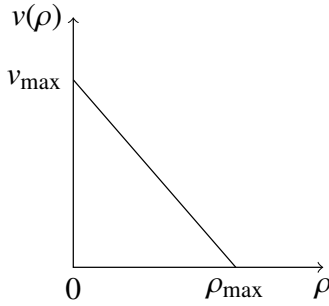


Figure 6: Speed of cars: linear decreasing function.

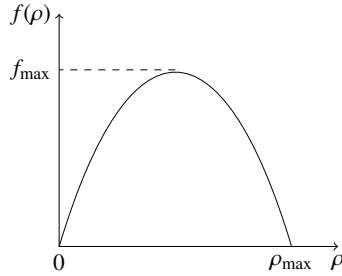


Figure 7: Fundamental diagram.

4.3.2 Traffic flow on a road network

The LWR model has been used extensively as the starting point for macroscopic traffic flow models. This model has been, subsequently, extended to the network case, see [22,47,49]. In these works, the road network is described as a graph with a finite number of vertices and edges. Each vertex describes a road junction and each edge a road. The first work dealing with traffic flow on networks dates back to the nineties when Holden and Risebro [65] introduced the concept of road network and traffic distribution at junctions. The problem at the junction J for j roads is solved maximizing a concave function of the fluxes of this form

$$\sum_{\text{roads } j \text{ at } J} g\left(\frac{f(\rho_j)}{f_{\max}}\right).$$

Their work, which considers only unidirectional networks, has then been extended for general networks by Coclite, Garavello and Piccoli in [22].

In [22], the road network is described as a graph and it can be uniquely determined by a couple (I, J) where I represents a finite collection of edges describing the roads and J a finite collection of nodes representing the road junctions. On each edge the LWR model describes the evolution of the cars density and coupling conditions are given at the nodes to correctly distribute the traffic through the junction. Let us consider a network (I, J) with a single junction J and N incoming roads and M outgoing ones, see Figure 8. Each road can be described with an interval $I_l = [a_l, b_l]$ for $l = 1, \dots, N, N+1, \dots, N+M$. On each road consider the equation

$$\partial_t \rho_l + \partial_x f(\rho_l) = 0, \quad l = 1, \dots, N+M, \quad (13)$$

where $\rho_l = \rho_l(t, x) \in [0, \rho_{\max}]$, $(t, x) \in \mathbb{R}^+ \times I_l$ for $l = 1, \dots, N+M$ is the density of cars in the road I_l , $f : [0, \rho_{\max}] \rightarrow \mathbb{R}$ is the flux function and it is taken equal to $f = \rho_l v(\rho_l)$. To distribute the traffic at the junction the following assumptions are made:

- The drivers have some prescribed preferences that means that there are some fixed coefficients which distribute the traffic from the incoming roads to the outgoing ones.
- The drivers choose to maximize the flux through the junction, respecting the prescribed preferences.

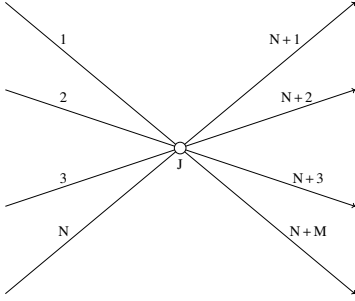


Figure 8: An example of a graph representing a road junction.

Moreover, in order to fulfill the conservation of ρ at J , mass must be conserved, i.e., the total incoming flux must be equal to the outgoing one:

$$\sum_{i=1}^N f(\rho_i(t, b_i-)) = \sum_{j=N+1}^{N+M} f(\rho_j(t, a_j+)). \quad (14)$$

A traffic distribution matrix is introduced to distribute the traffic among the incoming and outgoing roads.

4.4 Micro-macro models

It is possible to extend the LWR model in order to include many features of traffic flow. Many works that go in this direction have been published in the last years. One particular line of research has been focusing on how to model the effects of a bottleneck among traffic. Bottlenecks may be generated by different reasons. We distinguish between fixed bottlenecks and moving ones. A fixed bottleneck is created by a reduction of the road capacity due to the presence of toll gates or road works, etc. The reduction in the capacity is fixed in one specific position. Moving bottlenecks are, instead, created by the presence of something that moves along the road that can be a slow and large vehicle (bus, trucks, etc.), a moving road construction site or a vehicle that moves with the purpose of controlling the rest of the vehicles. In this case it becomes necessary, not only, to be able to model the capacity reduction, but also to be able to track a single vehicle among the traffic flow.

Over the years several works have focused on modeling these effects. In the engineering framework, we recall the works by C. Daganzo and J.Laval [27, 28] and by L. Leclercq, J.-P. Lebacque, J. B. Lesort and F. Giorgi [52, 53, 80]. All these works are developed in the discrete setting. In the mathematical community, research has focused both on fixed and moving bottleneck [23, 78].

4.4.1 Modeling of a tollgate

Colombo and Goatin [23] model the effect of a tollgate on traffic flow by a conservation law with a time-dependent unilateral constraint. The problem reads

$$\begin{cases} \partial_t \rho + \partial_x f = 0 & (t, x) \in (\mathbb{R}^+, \mathbb{R}), \\ \rho(0, x) = \rho_0(x) & x \in \mathbb{R}, \\ f(\rho(t, 0)) \leq q(t), & t \in \mathbb{R}^+, \end{cases} \quad (15)$$

where $q(t)$ is the maximal flux allowed through the toll at time t .

4.4.2 Tracking a car among traffic flow

As mentioned above, in many cases it might be useful to track a vehicle among traffic flow. This is quite hard to do with macroscopic models that consider traffic as a whole. On the other hand, tracking all vehicles like in the microscopic approach is quite heavy if our aim is to know the position of one driver, which is why some researchers have tried to couple the two approaches in order to have the advantages of both. The first work that goes in this direction is the one by Colombo and Marson [24]. Here, the main traffic flow is described by the LWR model while the ordinary differential equation (16) accounts for the trajectory of a single driver moving at average speed.

$$\begin{cases} \dot{y} = v(\rho(t, y)) \\ y(0) = y_0, \end{cases} \quad (16)$$

where y is the position of the driver and it is supposed that the driver is influenced by the traffic surrounding him but the single driver does not influence the traffic.

The ODE is considered in Filippov's sense [43, §4], due to the discontinuity of the right hand side.

We remark that the model considered in [24] introduces a weak coupling between the LWR and the ODE imposing only a "one-way" influence. In particular, the PDE is independent of the ODE solution.

4.4.3 Moving bottlenecks

In this subsection, we will describe micro-macro models that were introduced in the literature to describe the phenomenon that happens when a vehicle with a different dynamics is introduced in the flow of traffic. Most of these are for a large and slow vehicle which has dynamics significantly different from the rest of the traffic. From a modeling standpoint this results in having to describe them with different tools. Nowadays, these models could be also used to describe what happens when we have autonomous vehicles with low penetration rate. In fact, the microscopic dynamics is a tool to describe what happens for vehicles that behave differently than the rest and the interaction term, be it a mollifier or a constraint, could be tuned to describe how an autonomous vehicle interacts with the rest of the flow.

Moving bottleneck. The first mathematical model that describes the interaction between the traffic flow and a slower vehicle is due to Lattanzio, Maurizi and Piccoli [79]. They introduce a fully coupled model where the vehicle described by the ODE interacts with the whole traffic flow, obtaining a micro-macro coupled model. In particular, the situation that the authors refer to is that of a large and slow vehicle that generates a drop of capacity in the road. The model reads

$$\begin{cases} \partial_t \rho + \partial_x f(x, y(t), \rho) = 0, \\ \rho(0, x) = \rho_0(x), \\ \dot{y} = \omega(\rho(t, y)), \\ y(0) = y_0, \end{cases} \quad (17)$$

where the flux function $f(x, y(t), \rho) = \rho v(\rho) \varphi(x - y(t))$, with $\varphi(\xi)$ being a mollifier representing the capacity drop of car flow. The speed $\omega(\rho) : [0, \rho_{\max}] \rightarrow [0, +\infty)$ is a smooth and decreasing function describing the slower vehicle. Existence of solutions is proved with the fractional step method.

The above model is then extended in [50] to several routes (for example of a bus) on a closed path on networks. Traffic flow is described by the following initial-boundary value problem

$$\begin{cases} \partial_t \rho + \partial_x f(x, y_1, \dots, y_N, \rho) = g(t, x, \rho), \\ \rho(0, x) = \rho_0(x), \\ \rho(t, 0) = \rho(t, L), \end{cases} \quad (18)$$

where $y_i = y_i(t)$ is the position of the i -th discrete vehicle. The flux function f is given by $f(x, y_1, \dots, y_N, \rho) = \rho \cdot v(\rho) \cdot \Phi(x, y_1, \dots, y_N)$. The function $\Phi(y_1, \dots, y_N) = \min_i \varphi(x - y_i(t))$, with φ the mollifier as in (17), is responsible for the coupling with the ODEs and $g(t, x, \varphi)$ is a source term that accounts for the junctions. This macroscopic model is then coupled with a microscopic model of a follow-the-leader type, where the behavior of the drivers of the vehicles is influenced by the behavior of the drivers ahead. The coupling guarantees that the velocities of buses are at most the flow velocity, thus depending on the surrounding density, and become the maximal possible velocity when the effects of vehicles ahead are negligible.

Constraint model. The aim of this section is to describe the phenomena caused by the presence of a slower vehicle (like a bus, or a purposely slower vehicle) in a car flow. Since the macroscopic description of the traffic does not allow to consider single vehicles, we consider the slower vehicle as a mobile obstacle that reduces the capacity of the road generating a moving bottleneck for the surrounding traffic. This situation can be modeled by a PDE-ODE strongly coupled system consisting of a scalar conservation law with moving flux constraint accounting for traffic evolution and an ODE describing the slower vehicle motion, i.e.,

$$\begin{cases} \partial_t \rho + \partial_x f = 0, & (t, x) \in \mathbb{R}^+ \times \mathbb{R}, \\ \rho(0, x) = \rho_o(x), & x \in \mathbb{R}, \\ f(\rho(t, y(t))) - \dot{y}(t) \rho(t, y(t)) \leq \frac{\alpha \rho_{\max}}{4v_{\max}} (v_{\max} - \dot{y}(t))^2 & t \in \mathbb{R}^+, \\ \dot{y}(t) = \omega(\rho(t, y(t))), & t \in \mathbb{R}^+, \\ y(0) = y_o. & \end{cases} \quad (19)$$

The traffic evolution is described by a scalar hyperbolic conservation law (11) with the flux given by the following relation

$$f = \rho v(\rho),$$

where v is a smooth decreasing function denoting the mean traffic speed and here set to be $v(\rho) = v_{\max}(1 - \frac{\rho}{\rho_{\max}})$, v_{\max} being the maximal velocity allowed on the road.

The slower vehicle does not behave like cars, hence, it cannot be modeled in the same way. We represent a single vehicle such that we can track its trajectory at all times. When it is possible, the vehicle will move at its own maximal speed which, we denote as $V_b < v_{\max}$. When the surrounding traffic is too dense the vehicle will adapt its velocity to that one of the cars, so it will not be possible for the slower vehicle to overtake the cars, see Figure 9.

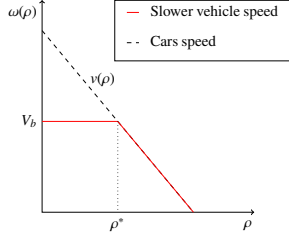


Figure 9: Slower vehicle and cars speed.

From a mathematical point of view, the velocity of the vehicle can be described by the following function:

$$\omega(\rho) = \begin{cases} V_b & \text{if } \rho \leq \rho^* \doteq \rho_{\max}(1 - \frac{V_b}{v_{\max}}), \\ v(\rho) & \text{otherwise,} \end{cases} \quad (20)$$

and the slower vehicle trajectory is described by the following ODE

$$\dot{y}(t) = \omega(\rho(t, y(t)+)) \quad (21)$$

where y denotes the position of the vehicle.

To describe the interaction between the slower vehicle and the traffic we consider the vehicle as a mobile obstacle, i.e., as a moving restriction of the road. The situation is the following: the cars in the upstream and downstream with respect to the slower vehicle behave normally while on the side of the slower vehicle the road capacity is reduced, generating a bottleneck, see Figure 10. This discontinuity moves at the vehicle speed. To

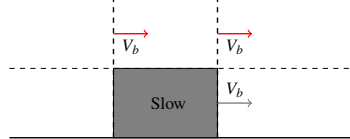


Figure 10: Moving bottleneck.

better capture the influence of the slower vehicle, we choose to study the problem in the slower vehicle reference frame. This means setting $X = x - y(t)$. In this coordinate system the velocity of the slower vehicle is equal to zero. As a consequence the conservation law can be rewritten as:

$$\partial_t \rho + \partial_X (f - \dot{y}\rho) = 0. \quad (22)$$

The corresponding constraint on the flux can be written as

$$f(\rho(t, y(t))) - \dot{y}(t)\rho(t, y(t)) \leq \frac{\alpha \rho_{\max}}{4v_{\max}} (v_{\max} - \dot{y}(t))^2, \quad (23)$$

with the constant coefficient $\alpha \in]0, 1[$ giving the reduction rate of the road capacity due to the presence of the slower vehicle. Indeed, let $F_\alpha : [0, \alpha \rho_{\max}] \rightarrow \mathbb{R}^+$ be the rescaled flux function describing the reduced flow at $x = y(t)$, i.e.

$$F_\alpha(\rho) = V\rho \left(1 - \frac{\rho}{\alpha \rho_{\max}}\right),$$

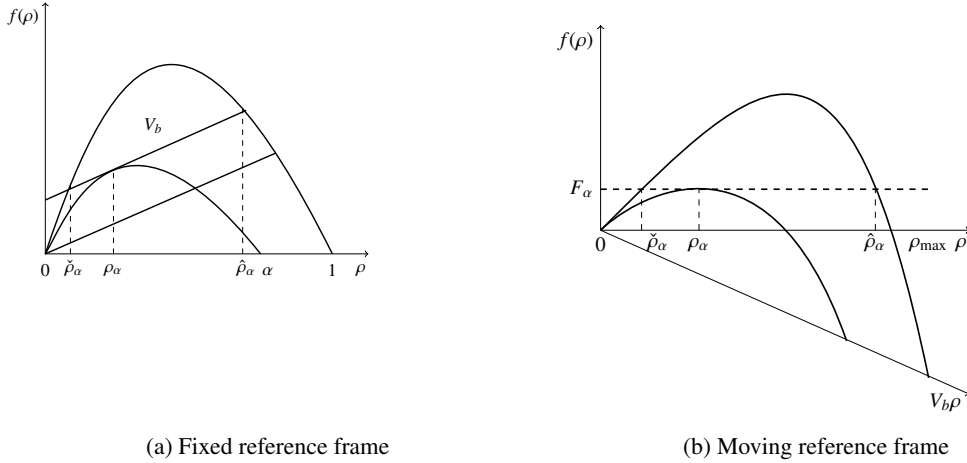


Figure 11: Flux functions for $\dot{y} = V_b$. The big fundamental diagram describes the whole road and, the smaller one, the constrained flux at the slower vehicle location.

and $\rho_\alpha \in]0, \alpha\rho_\alpha) = \dot{y}$, i.e.

$$\rho_\alpha = \frac{\alpha\rho_{\max}}{2} \left(1 - \frac{\dot{y}}{v_{\max}}\right),$$

see Figure 11. Therefore, the right-hand side of (23) is given by

$$F_\alpha(\rho_\alpha) - \dot{y}\rho_\alpha = \frac{\alpha\rho_\alpha}{4V}(V - \dot{y}(t))^2.$$

Note that inequality (23) is always satisfied if $\dot{y}(t) = v(\rho)$, since the left hand side is 0. Moreover, it is well defined even if ρ has a jump at $y(t)$ because of the Rankine-Hugoniot conditions. This constraint describes mathematically the reduction of capacity of the road due to the presence of the slower vehicle.

Autonomous vehicles in human traffic can be represented by this last class of models where the microscopic dynamics can describe the trajectory of an autonomous vehicle and the constraint or the mollifier represent its interaction with the human flow. Moreover, this representation becomes more pertinent if the autonomous vehicle is used as a control vehicle for the rest of the flow.

5 Eulerian to Lagrangian traffic estimation & control

As traffic flow begins to change due to the introduction of connected and autonomous vehicles, opportunities for traffic estimation and control are evolving. In this section we summarize some of the main works on traffic estimation and control. Here we restrict our focus to highway methods to simplify the discussion. Historically, traffic estimation and control algorithms have been realized and implemented using Eulerian sensors and actuators, i.e., sensors and actuators that are at fixed locations on the roadway. However, with the widespread introduction of GPS devices in vehicles that offer sensing and connectivity, a fundamental shift occurred in traffic estimation towards one relying on Lagrangian or mobile sensing. Now, as vehicles become automated, we are witnessing new opportunities for traffic control, shifting from Eulerian control algorithms based on ramp metering and variable speed limits to one in which automated vehicles act as Lagrangian control devices.

5.1 From Eulerian to Lagrangian traffic estimation

The foundations of Eulerian traffic estimation for freeways hinge on the adoption of a conservation law describing the evolution of traffic density on a freeway section, e.g., via a macroscopic PDE model such as the LWR (11) [85, 115].

Generally, traffic state estimation problems are considered in the sequential setting using a state space form of the model and measurement system:

$$\begin{aligned} x^{n+1} &= f(x^n, \omega^n) \\ z^n &= h(x^n, v^n), \end{aligned} \tag{24}$$

where x^n is the traffic state time step n (e.g., a vector of the traffic density on the stretch of road), and f is the model describing traffic flow and its evolution from one time increment to the next one. The random variable ω^n is the model noise representing the one time step prediction error of the model, which is often assumed to be zero mean, Gaussian, and white. In the measurement equation, the function h is the observation equation which relates the state vector x^n to the measurements z^n received at time n . It has an associated measurement noise random variable v^n , which characterizes the performance of the sensor.

Historically, traffic sensors such as inductive loop detectors directly measured vehicle counts, and indirectly calculated traffic densities and velocities, e.g., by exploiting the average length of a vehicle and the percent of time the sensor was occupied. Modern radar-based sensors produce high quality speed and count data across all lanes of a freeway. GPS devices in vehicles measure individual vehicle speeds very precisely, however they can suffer from sample approximation errors if the state vector tracks an aggregate quantity such as density or average speed, and only a point measurement from a small number of vehicles are obtained on the roadway of interest.

The sequential traffic state estimation problem, i.e., where one estimates x^n using measurements $Z^n = \{z^1, \dots, z^n\}$, and the system (24) were introduced through the works of Gazis and Knapp [51] and Setzo and Gazis [134] in the 1970's, who were the first to consider the use of Kalman filtering for road monitoring applications. Moreover, through a series of experiments conducted in the Lincoln Tunnel in New York City, a system was implemented and used to track the density of vehicles in the tunnel. Some early works considered simplistic traffic dynamics by today's standards, e.g., including a single state linear model, but extensions were quickly proposed and a variety of models and filtering extensions were developed.

While many works considered variants of traffic flow models built primarily on conservation of vehicles (e.g., in the spirit of the LWR model (11)), a notable line of work explored the problem of traffic estimation where the dynamics are governed Payne's macroscopic model [107], as used for a variety of Kalman-based estimators [26, 104, 144, 145].

Regardless of the underlying macroscopic traffic flow model employed, there are several challenges that make the state estimation problem challenging to directly apply Kalman filtering based methods. These include the fact that the discretized versions of the LWR model (e.g., the cell transmission model [29, 30], which is a finite volume scheme based on Godunov's method [54]) are nonlinear and nondifferentiable [15]. This has motivated the use of a variety of nonlinear Kalman based estimators [69, 92, 129, 130, 148] and particle filtering [91, 93, 94, 111, 117, 141, 143].

Beyond practical applications and numerical case studies, there are several works that investigate the properties of macroscopic flow model based traffic state estimators. In [98, 128], the discretized LWR is recast as a switched linear system under mild assumptions, and is referred to as the *switching mode model* (SMM). Each mode in the model corresponds to a traffic configuration defined by conditions of traffic upstream and downstream on the roadway stretch (e.g., free-flowing traffic upstream, and congested traffic downstream). In each mode, the state space model is linear and as a result it is straightforward to determine which modes are observable and unobservable. Importantly, it is shown that when a shock exists on the roadway (i.e., free flowing traffic upstream connects to traffic congestion downstream), the traffic state cannot be observed from boundary measurements of the traffic state alone. This negative result hinders many practical applications, such as queue warning systems that alert drivers about the distance to the queue ahead. The use of the SMM model in traffic estimation resulted in the mixture Kalman filter approach developed in [128] to estimate traffic densities to support ramp metering.

A brief summary of other important theoretical discussions on model based traffic estimation are as follows. The work [97] analyzed the performance of a noise-free Luenberger observer for traffic estimation based on the SMM, which is the first work to provide theoretical performance analysis for any traffic estimator under both observable and unobservable scenarios. The method drops the measurement feedback when the traffic state is unobservable, e.g., when a shock exists in the domain, which allows for the sum over the state variables of the estimation error to be conserved. Intuitively, if the boundary measurements are exact and the traffic dynamic is a conservation law, then the sum of the errors must also be conserved in the domain. A similar strategy is adopted in [140] in which an open loop predictor is used in unobservable regimes.

While the results [97, 140] illustrate the potential theoretical benefits of dropping the measurement feedback of the estimator when the system mode is unobservable, it was later shown that the choice could ultimately lead to non-physical estimates in some circumstances (e.g., state estimates that exceed the maximum density permissible on the roadway) [132]. The overall performance of an estimator that considers measurement feedback as well

as switches between observable traffic modes and unobservable modes was provided in [132], which proved the boundedness of the mean estimation error of a traffic estimator.

We also note a Gaussian approximation of a stochastic extension of the LWR model was considered in [69], and as a result it was possible to prove the stochastic observability of the system. The result requires a warm-up period with initially free flowing traffic conditions (a realistic assumption given that eventually most roads become free flowing late at night). In another line of work, the bound of the state estimates are analyzed using *set-valued estimation* [76], given assumptions that model parameters and measurement and process noises are bounded known intervals. Intervals which are guaranteed to include the true states can then be estimated [77].

Note that the theoretical performance analysis of traffic estimators at transportation networks with junctions described in Section 4.3.2 has fewer results. The set-valued estimation approach [77], and the work [131] deals with traffic dynamics at junctions, and all the results in [25, 69, 97, 140] are restricted to one-dimensional road stretches without considering junction dynamics.

While the problem of traffic state estimation has evolved considerably both in the fidelity of the modeling and the filtering algorithms, a major transformation occurred with the introduction of GPS-based datastreams that are now widely used in many commercial traffic estimation systems around the world. Restricting to the model based estimators, most of the approaches modify the state estimation problem to a time varying measurement equation, where the number of measurements and the mapping of the state vector to the measurements evolve in time as the sensors move along the roadway. This is the approach considered in [33, 62, 63, 146, 147], as well as the work [7], which considers a differentially private formulation to prevent tracking attacks. An interesting alternative formulation considers transforming the macroscopic model into Lagrangian coordinates, and applying a filter on the transformed model. This is the approach considered in [151]. In [25], the local observability around an equilibrium traffic state is studied using a Lagrangian formulation of the traffic model.

As connected and automated vehicles emerge, there is a growing interest to use them as measurement sources for traffic estimation problems. For example the works [10, 11, 116] consider the problem of traffic estimation under the assumption that the velocity field along the roadway is a known time-varying parameter, and it is assumed to be provided by a high penetration rate of connected and automated vehicles in the traffic stream. It also assumes the automated vehicles have the same driving characteristics as human drivers do (e.g., they have the same average following distance in congestion, and there is no bulk overtaking by humans or automated vehicles). If instead the AVs are treated as a distinct flow, a multi-class model which is a generalization of the *Aw Rascle Zhang* (ARZ) [8, 152] model can be proposed, for which standard filtering approaches such as the particle filter can be applied [142].

Approaches that consider Lagrangian tracers (e.g., connected and automated vehicles) based on micro-macro models are now beginning to be developed. For example, in [37], autonomous vehicles (described by an ODE) act as tracer vehicles in the bulk flow (described by a PDE). The main result is to prove theoretically and show numerically how to reconstruct the correct traffic density using only the measurements from the autonomous vehicles.

5.2 From fixed to mobile traffic control

Given the nature of freeways, the number of control possibilities has historically been rather restricted compared to urban networks complete with traffic signal infrastructure. However, given the prevalence of congestion on freeways, a concerted effort has been made to develop approaches to control traffic flow to reduce congestion. The two major classes of approaches are based on actuation at the freeway on-ramps through ramp metering lights, and actuation on the freeway itself by dynamically changing the speed limits in variable speed limit control. Both ramp metering and variable speed limits are used to restrict inflow to a downstream section of the roadway, and can be used concurrently [60].

Ramp metering strategies are effective because when the roadway is near capacity (the maximum flow f^{\max} in Figure 7), a small addition of drivers can exceed the downstream capacity of a bottleneck, triggering congestion. Once congestion caused by a bottleneck is triggered, it can only be removed by reducing the inflow from the upstream, thereby reversing the growth of congestion. Moreover, in empirical data, one commonly observes a capacity drop phenomenon [58]. The capacity drop refers to the observation that the maximum outflow of a congested freeway is less than the maximum outflow of an uncongested freeway. In other words, empirical fundamental diagrams have a discontinuity at the critical density. This implies that the roadway must remain free-flowing in order to maximize the throughput of the roadway, and holding back a few drivers at ramps to the benefit of all of the drivers already on the freeway is a good strategy to achieve the highest throughput.

One limitation of ramp metering is that the total number of vehicles that can be stored on ramps is restricted (limited by the length of the ramp). If the meters are too restrictive, the congestion on the ramps can spill back onto the surface street network, limiting the effectiveness of urban traffic signal control strategies.

To overcome the fact that the ramp meters can quickly saturate due to the limited storage available on ramps, variable speed limits have been proposed as a viable alternative or additional control strategy. Variable speed limits are effective because they change the shape of the fundamental diagram in the section where they are applied, thereby slightly slowing traffic far upstream of a bottleneck to reduce the flow headed downstream towards the bottleneck. Because it has the potential to actuate all vehicles on the mainline, it can be quite effective at influencing the traffic flow. Currently, the major limitation of variable speed limit control algorithms in some geographies is due to the fact that it depends on human drivers to be compliant with the dynamically posted speed. In locales where the speed is advisory rather than a requirement, or where enforcement rates are low, the compliance rate can be reduced.

A seminal review of ramp metering approaches can be found in [106], and a more general survey on variable speed limits, ramp metering and surface street control are found in [105]. The major recent developments in freeway traffic control can be found in the book [42], including the use of connected and autonomous vehicles to implement variable speed limits, e.g., as in [59, 73].

While the concept to use connected and automated vehicles within the classical freeway traffic management strategies is relatively recent, the development of connected and automated vehicle systems has been closely linked with traffic management applications. For example, completely automated highways have been considered [12, 41]. We do not summarize the development of vehicle automation systems (e.g., [122]) which can already be found in the reviews [18, 66, 121, 137].

Based on the substantial growth in commercially deployed automated vehicle technologies such as driver assist systems, as well as the development of highly automated vehicle programs, the possibilities of using automated vehicles themselves as Lagrangian traffic controllers is now within reach. For example, connected and automated vehicles have the potential to dramatically increase or deduce the roadway capacity, depending on how closely they are able to safely follow the vehicle ahead [34]. This is because the traffic flow (typically measured in units such as veh/hr) is the inverse of the average vehicle time headway (often described in units of sec/veh). Passive autonomous vehicles leaving large headways can reduce roadway capacity, while connected and automated vehicles have the possibility of doubling or tripling the capacity of a lane of traffic.

In addition to influencing the total throughput, automated vehicles also have the potential to influence the string stability of the traffic flow. Commonly referred to as jamitons, stop-and-go waves, or phantom traffic jams [44], the nature of human driving can lead to traffic jams that seemingly occur without a cause but are in fact due to an instability in the car following behavior of the driver. This was demonstrated experimentally in the seminal experiments of [127], in which a stop and go wave appears on a circular track with no lane changes or geometric bottlenecks. Given that automated vehicles have different driving dynamics compared to humans, they also offer the possibility to reduce these phantom jams.

Considering both traffic flow stability and throughput, a variety of modeling and analysis efforts, typically at the microscopic modeling scale as in (8) have considered how these vehicles can influence traffic dynamics [16, 16, 32, 39, 81, 83, 100, 101, 123, 135, 137]. Building on the experimental work [127], it has been recently experimentally demonstrated that autonomous vehicles at penetration rates as low as 5% can effectively eliminate the presence of phantom traffic jams caused by human drivers [126]. More broadly, the interest in determining the potential benefits of automated driving systems on the traffic flow has been an ongoing research focus for the vehicular control and traffic engineering communities [16, 31, 32, 35, 40, 72, 123, 136, 137].

From an analysis and design perspective, significant progress has been made to create control laws in which a collection of automated vehicles under the same control laws is string stable [1, 13, 67, 82, 84, 96, 103, 112, 121, 133]. We note that constant spacing policies (i.e., where each vehicle maintains a fixed distance to the vehicle ahead) lead to string unstable platoons of vehicles [71, 90, 119]. In contrast, if it is not necessary to maintain a fixed spacing, one can adopt a constant time-headway policy that makes it possible to maintain string stability [68, 84]. These constant time headway policies serve as a basis for many *adaptive cruise control* ACC implementations.

We also note that although there are many positive findings about the potential benefit of Society of Automotive Engineers (SAE) level 1 automated vehicles such as ACC, the performance of commercial automation systems is less well understood. Preliminary studies including [56, 57, 74] indicate that current systems may have room for additional improvement from a string stability perspective, notwithstanding other design constraints such as safety and rider comfort [149].

One can enhance each vehicle with connectivity to other vehicles in the platoon to form dense platoons of vehicles which leave very small gaps. The benefits of so called connected adaptive cruise control systems have

been experimentally demonstrated [95, 99, 110], even in the presence of human vehicles [70].

6 Conclusions

Due to the ever-improving sensing, communication, computation, and actuation capabilities at all scales of vehicular transportation systems, there are a variety of opportunities to link advances on individual vehicles to societal scale improvements that ameliorate safety while reducing emissions, fuel consumption, and traffic congestion. As a result, as research in these areas continues to mature, it will become crucial for these sometimes silo-ed areas to interact with one another to truly achieve these promised safety and efficiency benefits. This overview is meant to provide the starting directions on some of the emerging areas that connect across these different scales systems and highlight the growing convergence of mathematical modeling, cyber physical systems, decision sciences, and transportation science.

References

- [1] A. Alam, B. Besselink, V. Turri, J. Martensson, and K. H. Johansson. Heavy-duty vehicle platooning for sustainable freight transportation: A cooperative method to enhance safety and efficiency. *IEEE Control Systems*, 35(6):34–56, 2015.
- [2] M. Althoff and J. M. Dolan. Set-based computation of vehicle behaviors for the online verification of autonomous vehicles. In *2011 14th International IEEE Conference on Intelligent Transportation Systems (ITSC)*, pages 1162–1167. IEEE, 2011.
- [3] M. Althoff and J. M. Dolan. Online verification of automated road vehicles using reachability analysis. *IEEE Transactions on Robotics*, 30(4):903–918, 2014.
- [4] M. Althoff and D. Gribenouik. Implementation of interval arithmetic in {CORA} 2016. In *Proc. of the 3rd International Workshop on Applied Verification for Continuous and Hybrid Systems*, 2016.
- [5] A. D. Ames, S. Coogan, M. Egerstedt, G. Notomista, K. Sreenath, and P. Tabuada. Control barrier functions: Theory and applications. *arXiv preprint arXiv:1903.11199*, 2019.
- [6] A. D. Ames, J. W. Grizzle, and P. Tabuada. Control barrier function based quadratic programs with application to adaptive cruise control. In *53rd IEEE Conference on Decision and Control*, pages 6271–6278. IEEE, 2014.
- [7] H. Andre and J. Le Ny. A differentially private ensemble kalman filter for road traffic estimation. In *2017 IEEE International Conference on Acoustics, Speech and Signal Processing (ICASSP)*, pages 6409–6413. IEEE, 2017.
- [8] A. Aw and M. Rascle. Resurrection of second order models of traffic flow. *SIAM J. Appl. Math.*, 60:916–944, 2000.
- [9] M. Bando, K. Hasebe, A. Nakayama, A. Shibata, and Y. Sugiyama. Dynamical model of traffic congestion and numerical simulation. *Physical Review E*, 51(2):1035–1042, 1995.
- [10] N. Bekiaris-Liberis, C. Roncoli, and M. Papageorgiou. Highway traffic state estimation with mixed connected and conventional vehicles using speed measurements. In *Proceedings of the IEEE International Conference on Intelligent Transportation Systems*, pages 2806–2811, 2015.
- [11] N. Bekiaris-Liberis, C. Roncoli, and M. Papageorgiou. Highway traffic state estimation with mixed connected and conventional vehicles. *IEEE Transactions on Intelligent Transportation Systems*, 99:1–14, 2016.
- [12] J. G. Bender. An overview of systems studies of automated highway systems. *IEEE Transactions on Vehicular Technology*, 40(1):82–99, 1991.
- [13] B. Besselink and K. H. Johansson. String stability and a delay-based spacing policy for vehicle platoons subject to disturbances. *IEEE Transactions on Automatic Control*, 2017.

- [14] R. Bhadani, B. Piccoli, B. Seibold, J. Sprinkle, and D. B. Work. Dissipation of emergent traffic waves in stop-and-go traffic using a supervisory controller. In *57th IEEE Conference on Decision and Control*, volume 57, 2018.
- [15] S. Blandin, A. Couque, A. Bayen, and D. B. Work. On sequential data assimilation for scalar macroscopic traffic flow models. *Physica D: Nonlinear Phenomena*, 241(17):1421–1440, 2012.
- [16] A. Bose and P. A. Ioannou. Analysis of traffic flow with mixed manual and semiautomated vehicles. *IEEE Transactions on Intelligent Transportation Systems*, 4(4):173–188, 2003.
- [17] M. Brackstone and M. McDonald. Car-following : a historical review. *Transportation Research Part F: Traffic Psychology and Behaviour*, 2(4):181–196, 1999.
- [18] M. Buehler, K. Iagnemma, and S. Singh. *The DARPA urban challenge: autonomous vehicles in city traffic*, volume 56. Springer, 2009.
- [19] R. E. Chandler, R. Herman, and E. W. Montroll. Traffic Dynamics: Studies in Car Following. *Operations Research*, 6(2):165–184, 1958.
- [20] Y. Chen, H. Peng, and J. Grizzle. Obstacle avoidance for low-speed autonomous vehicles with barrier function. *IEEE Transactions on Control Systems Technology*, 26(1):194–206, 2017.
- [21] Y. Chitour and B. Piccoli. Traffic circles and timing of traffic lights for cars flow. *Discrete and Continuous Dynamical Systems-Series B*, 5(3):599–630, may 2005.
- [22] G. M. Coclite, M. Garavello, and B. Piccoli. Traffic Flow on a Road Network. *SIAM Journal on Mathematical Analysis*, 36(6):1862–1886, jan 2005.
- [23] R. M. Colombo and P. Goatin. A well posed conservation law with a variable unilateral constraint. *J. Differential Equations*, 234(2):654–675, 2007.
- [24] R. M. Colombo and A. Marson. A Hölder continuous ODE related to traffic flow. *Proc. Roy. Soc. Edinburgh Sect. A*, 133(4):759–772, 2003.
- [25] S. Contreras, S. Agarwal, and P. Kachroo. Quality of traffic observability on highways with lagrangian sensors. *IEEE Transactions on Automation Science and Engineering*, 2017.
- [26] M. Cremer and M. Papageorgiou. Parameter identification for a traffic flow model. *Automatica*, 17(6):837–843, 1981.
- [27] C. Daganzo and J. A. Laval. Moving bottlenecks: A numerical method that converges in flows. *Transportation Research Part B*, 39:855–863, 2004.
- [28] C. Daganzo and J. A. Laval. On the numerical treatment of moving bottlenecks. *Transportation Research Part B*, 39:31–46, 2005.
- [29] C. F. Daganzo. The cell transmission model: A dynamic representation of highway traffic consistent with the hydrodynamic theory. *Transportation Research Part B: Methodological*, 28(4):269–287, 1994.
- [30] C. F. Daganzo. The cell transmission model, part II: network traffic. *Transportation Research Part B: Methodological*, 29(2):79–93, 1995.
- [31] S. Darbha and K. R. Rajagopal. Intelligent cruise control systems and traffic flow stability. *Transportation Research Part C: Emerging Technologies*, 7(6):329 – 352, 1999.
- [32] L. C. Davis. Effect of adaptive cruise control systems on traffic flow. *Physical Review E*, 69(6):066110, 2004.
- [33] C. De Fabritiis, R. Ragona, and G. Valenti. Traffic estimation and prediction based on real time floating car data. In *Proceedings of the IEEE Conference on Intelligent Transportation Systems*, pages 197–203, 2008.

- [34] A. I. Delis, I. K. Nikolos, and M. Papageorgiou. Macroscopic traffic flow modeling with adaptive cruise control: Development and numerical solution. *Computers & Mathematics with Applications*, 70(8):1921–1947, 2015.
- [35] A. I. Delis, I. K. Nikolos, and M. Papageorgiou. Simulation of the penetration rate effects of acc and cacc on macroscopic traffic dynamics. In *Proceedings of the 2016 IEEE 19th International Conference on Intelligent Transportation Systems (ITSC)*, pages 336–341. IEEE, 2016.
- [36] M. L. Delle Monache and P. Goatin. Scalar conservation laws with moving constraints arising in traffic flow modeling: An existence result. *Journal of Differential Equations*, 257(11):4015–4029, 2014.
- [37] M. L. Delle Monache, T. Liard, B. Piccoli, R. E. Stern, and D. Work. Traffic reconstruction using autonomous vehicles. working paper or preprint, Sept. 2018.
- [38] M. L. Delle Monache, J. D. Reilly, S. Samaranayake, W. Krichene, P. Goatin, and A. M. Bayen. A PDE-ODE Model for a Junction with Ramp Buffer. *SIAM Journal on Applied Mathematics*, 74(1):22–39, jan 2014.
- [39] C. Diakaki, M. Papageorgiou, I. Papamichail, and I. Nikolos. Overview and analysis of vehicle automation and communication systems from a motorway traffic management perspective. *Transportation Research Part A: Policy and Practice*, 75:147–165, 2015.
- [40] R. A. Dollar and A. Vahidi. Efficient and collision-free anticipative cruise control in randomly mixed strings. *IEEE Transactions on Intelligent Vehicles*, 3(4):439–452, 2018.
- [41] R. E. Fenton and R. J. Mayhan. Automated highway studies at the Ohio State University—an overview. *IEEE transactions on Vehicular Technology*, 40(1):100–113, 1991.
- [42] A. Ferrara, S. Sacone, and S. Siri. *Freeway traffic modelling and control*. Springer, 2018.
- [43] V. V. Filippov. *Ordinary differential equations with discontinuous right-hand sides*, volume 30. Kluwer academic Publisher, 1994.
- [44] M. R. Flynn, A. R. Kasimov, J.-C. Nave, R. R. Rosales, and B. Seibold. Self-sustained nonlinear waves in traffic flow. *Phys. Rev. E*, 79(5):056113, 2009.
- [45] D. Fridovich-Keil, S. L. Herbert, J. F. Fisac, S. Deglurkar, and C. J. Tomlin. Planning, fast and slow: A framework for adaptive real-time safe trajectory planning. In *2018 IEEE International Conference on Robotics and Automation (ICRA)*, pages 387–394. IEEE, 2018.
- [46] M. Garavello and P. Goatin. The Cauchy problem at a node with buffer. *Discrete and Continuous Dynamical Systems - Series A*, 32(6):1915–1938, feb 2012.
- [47] M. Garavello and B. Piccoli. Traffic Flow on a Road Network Using the Aw–Rascle Model. *Communications in Partial Differential Equations*, 31(2):243–275, jan 2006.
- [48] M. Garavello and B. Piccoli. *Traffic flow on networks*, volume 1. American institute of mathematical sciences Springfield, 2006.
- [49] M. Garavello and B. Piccoli. Conservation laws on complex networks. *Annales de l'Institut Henri Poincare (C) Analyse Non Linéaire*, 26(5):1925–1951, 2009.
- [50] I. Gasser, C. Lattanzio, and A. Maurizi. Vehicular traffic flow dynamics on a bus route. *Multiscale Model. Simul.*, 11(3):925–942, 2013.
- [51] D. C. Gazis and C. H. Knapp. On-line estimation of traffic densities from time-series of flow and speed data. *Transportation Science*, 5(3):283–301, 1971.
- [52] F. Giorgi. *Prise en compte des transports en commun de surface dans la modélisation macroscopique de l’écoulement du trafic*. PhD thesis, Institut National des Sciences Appliquées de Lyon, 2002.

- [53] F. Giorgi, L. Leclercq, and J. B. Lesort. A traffic flow model for urban traffic analysis: extensions of the LWR model for urban and environmental applications. In *Proceeding of the 15th International Symposium on Transportation and Traffic Theory*, pages 393–416, 2002.
- [54] S. Godunov. A difference method for the numerical calculation of discontinuous solutions of hydrodynamic equations. *Mathematics Sbornik*, 47(3):271–306, 1959.
- [55] B. D. Greenshields. A study of traffic capacity. *Proc. Highway Res. Bd.*, 14:448, 1935.
- [56] G. Gunter, D. Gloudemans, R. E. Stern, S. McQuade, R. Bhadani, M. Bunting, M. L. D. Monache, R. Lysicky, B. Seibold, J. Sprinkle, et al. Are commercially implemented adaptive cruise control systems string stable? *arXiv preprint arXiv:1905.02108*, 2019.
- [57] G. Gunter, C. Janssen, W. Barbour, R. Stern, and D. B. Work. A model based approach to determine string stability of adaptive cruise control systems using field data. *submitted to the IEEE Transactions on Intelligent Vehicles*, 2019.
- [58] F. L. Hall and K. Agyemang-Duah. Freeway capacity drop and the definition of capacity. *Transportation research record*, (1320), 1991.
- [59] Y. Han, D. Chen, and S. Ahn. Variable speed limit control at fixed freeway bottlenecks using connected vehicles. *Transportation Research Part B: Methodological*, 98:113–134, 2017.
- [60] A. Hegyi, B. De Schutter, and H. Hellendoorn. Model predictive control for optimal coordination of ramp metering and variable speed limits. *Transportation Research Part C: Emerging Technologies*, 13(3):185–209, 2005.
- [61] S. L. Herbert, M. Chen, S. Han, S. Bansal, J. F. Fisac, and C. J. Tomlin. Fastrack: A modular framework for fast and guaranteed safe motion planning. In *2017 IEEE 56th Annual Conference on Decision and Control (CDC)*, pages 1517–1522. IEEE, 2017.
- [62] J. C. Herrera and A. M. Bayen. Incorporation of lagrangian measurements in freeway traffic state estimation. *Transportation Research Part B: Methodological*, 44(4):460–481, 2010.
- [63] J.-C. Herrera, D. Work, R. Herring, J. Ban, Q. Jacobson, and A. Bayen. Evaluation of traffic data obtained via GPS-enabled mobile phones: the Mobile Century experiment. *Transportation Research Part C: Emerging Technologies*, 18(4):568–583, 2010.
- [64] M. Herty and A. Klar. Modeling, Simulation, and Optimization of Traffic Flow Networks. *SIAM Journal on Scientific Computing*, 25(3):1066–1087, jan 2003.
- [65] H. Holden and N. H. Risebro. A Mathematical Model of Traffic Flow on a Network of Unidirectional Roads. *SIAM Journal on Mathematical Analysis*, 26(4):999–1017, jul 1995.
- [66] P. Ioannou. *Automated highway systems*. Springer Science & Business Media, 2013.
- [67] P. Ioannou, Z. Xu, S. Eckert, D. Clemons, and T. Sieja. Intelligent cruise control: theory and experiment. In *Proceedings of the 32nd IEEE Conference on Decision and Control*, pages 1885–1890. IEEE, 1993.
- [68] P. A. Ioannou and C.-C. Chien. Autonomous intelligent cruise control. *IEEE Transactions on Vehicular technology*, 42(4):657–672, 1993.
- [69] S. E. Jabari and H. Liu. A stochastic model of traffic flow: Gaussian approximation and estimation. *Transportation Research Part B: Methodological*, 47:15–41, 2013.
- [70] I. G. Jin and G. Orosz. Connected cruise control among human-driven vehicles: Experiment-based parameter estimation and optimal control design. *Transportation Research Part C: Emerging Technologies*, 95:445–459, 2018.
- [71] M. R. Jovanovic and B. Bamieh. On the ill-posedness of certain vehicular platoon control problems. *IEEE Transactions on Automatic Control*, 50(9):1307–1321, 2005.

- [72] A. Kesting, M. Treiber, and D. Helbing. Enhanced intelligent driver model to access the impact of driving strategies on traffic capacity. *Philosophical Transactions of the Royal Society A: Mathematical, Physical and Engineering Sciences*, 368(1928):4585–4605, 2010.
- [73] B. Khondaker and L. Kattan. Variable speed limit: A microscopic analysis in a connected vehicle environment. *Transportation Research Part C: Emerging Technologies*, 58:146–159, 2015.
- [74] V. Knoop, M. Wang, I. Wilmink, M. Hoedemaeker, M. Maaskant, V. der Meer, et al. Platoon of sae level-2 automated vehicles on public roads: Setup, traffic interactions, and stability. *Transportation Research Record*, 2019.
- [75] S. Kousik, S. Vaskov, F. Bu, M. Johnson-Roberson, and R. Vasudevan. Bridging the gap between safety and real-time performance in receding-horizon trajectory design for mobile robots. *arXiv preprint arXiv:1809.06746*, 2018.
- [76] A. A. Kurzhanskiy. Set-valued estimation of freeway traffic density. *IFAC Proceedings Volumes*, 42(15):271–277, 2009.
- [77] A. A. Kurzhanskiy and P. Varaiya. Guaranteed prediction and estimation of the state of a road network. *Transportation research part C: emerging technologies*, 21(1):163–180, 2012.
- [78] C. Lattanzio, A. Maurizi, and B. Piccoli. Moving Bottlenecks in Car Traffic Flow: A PDE-ODE Coupled Model. *SIAM Journal on Mathematical Analysis*, 43(1):50–67, jan 2011.
- [79] C. Lattanzio, A. Maurizi, and B. Piccoli. Moving bottlenecks in car traffic flow: a PDE-ODE coupled model. *SIAM J. Math. Anal.*, 43(1):50–67, 2011.
- [80] J.-P. Lebacque, J. B. Lesort, and F. Giorgi. Introducing buses into first-order macroscopic traffic flow models. *Transportation Research Record*, 1644:70–79, 1998.
- [81] M. W. Levin and S. D. Boyles. A multiclass cell transmission model for shared human and autonomous vehicle roads. *Transportation Research Part C: Emerging Technologies*, 62:103 – 116, 2016.
- [82] W. Levine and M. Athans. On the optimal error regulation of a string of moving vehicles. *IEEE Transactions on Automatic Control*, 11(3):355–361, 1966.
- [83] K. Li and P. Ioannou. Modeling of traffic flow of automated vehicles. *IEEE Transactions on Intelligent Transportation Systems*, 5(2):99–113, 2004.
- [84] C.-Y. Liang and H. Peng. Optimal adaptive cruise control with guaranteed string stability. *Vehicle System Dynamics*, 32(4-5):313–330, 1999.
- [85] M. J. Lighthill and G. B. Whitham. On Kinematic Waves. II. A Theory of Traffic Flow on Long Crowded Roads. *Proceedings of the Royal Society A: Mathematical, Physical and Engineering Sciences*, 229(1178):317–345, 1955.
- [86] A. Liniger and J. Lygeros. Real-time control for autonomous racing based on viability theory. *IEEE Transactions on Control Systems Technology*, (99):1–15, 2017.
- [87] A. Majumdar and R. Tedrake. Robust online motion planning with regions of finite time invariance. In *Algorithmic Foundations of Robotics X*, pages 543–558. Springer, 2013.
- [88] A. Majumdar and R. Tedrake. Funnel libraries for real-time robust feedback motion planning. *The International Journal of Robotics Research*, 36(8):947–982, 2017.
- [89] A. Marigo and B. Piccoli. A Fluid Dynamic Model for T -Junctions. *SIAM Journal on Mathematical Analysis*, 39(6):2016–2032, jan 2008.
- [90] R. H. Middleton and J. H. Braslavsky. String instability in classes of linear time invariant formation control with limited communication range. *IEEE Transactions on Automatic Control*, 55(7):1519–1530, 2010.
- [91] L. Mihaylova and R. Boel. A particle filter for freeway traffic estimation. In *Proceedings of the IEEE Conference on Decision and Control*, pages 2106–2111, 2004.

- [92] L. Mihaylova, R. Boel, and A. Hegyi. An unscented Kalman filter for freeway traffic estimation. In *Proceedings of the 11th IFAC Symposium on Control in Transportation Systems*, pages 31–36, 2006.
- [93] L. Mihaylova, R. Boel, and A. Hegyi. Freeway traffic estimation within particle filtering framework. *Automatica*, 43(2):290–300, 2007.
- [94] L. Mihaylova, A. Hegyi, A. Gning, and R. Boel. Parallelized particle and Gaussian sum particle filters for large-scale freeway traffic systems. *IEEE Transactions on Intelligent Transportation Systems*, 13(1):36 – 48, 2012.
- [95] V. Milanés, S. E. Shladover, J. Spring, C. Nowakowski, H. Kawazoe, and M. Nakamura. Cooperative adaptive cruise control in real traffic situations. *IEEE Transactions on Intelligent Transportation Systems*, 15(1):296–305, 2014.
- [96] J. Monteil, M. Bouroche, and D. J. Leith. \mathcal{L}_2 and \mathcal{L}_{∞} stability analysis of heterogeneous traffic with application to parameter optimization for the control of automated vehicles. *IEEE Transactions on Control Systems Technology*, 2018.
- [97] I. Morarescu and C. Canudas de Wit. Highway traffic model-based density estimation. In *Proceedings of the American Control Conference*, volume 3, pages 2012–2017, 2011.
- [98] L. Munoz, X. Sun, R. Horowitz, and L. Alvarez. Piecewise-linearized cell transmission model and parameter calibration methodology. *Transportation Research Record*, (1965):183–191, 2006.
- [99] G. J. Naus, R. P. Vugts, J. Ploeg, M. J. van de Molengraft, and M. Steinbuch. String-stable CACC design and experimental validation: A frequency-domain approach. *IEEE Transactions on Vehicular Technology*, 59(9):4268–4279, 2010.
- [100] D. Ngoduy. Application of gas-kinetic theory to modelling mixed traffic of manual and ACC vehicles. *Transportmetrica*, 8(1):43–60, 2012.
- [101] D. Ngoduy. Instability of cooperative adaptive cruise control traffic flow: a macroscopic approach. *Communications in Nonlinear Science and Numerical Simulation*, 18(10):2838–2851, 2013.
- [102] P. Nilsson, O. Hussien, A. Balkan, Y. Chen, A. D. Ames, J. W. Grizzle, N. Ozay, H. Peng, and P. Tabuada. Correct-by-construction adaptive cruise control: Two approaches. *IEEE Transactions on Control Systems Technology*, 24(4):1294–1307, 2015.
- [103] G. Orosz, B. Krauskopf, and R. E. Wilson. Bifurcations and multiple traffic jams in a car-following model with reaction-time delay. *Physica D: Nonlinear Phenomena*, 211(3-4):277–293, 2005.
- [104] M. Papageorgiou. *Applications of Automatic Control Concepts to Traffic Flow Modeling and Control*. Springer-Verlag New York, Inc., Secaucus, NJ, USA, 1983.
- [105] M. Papageorgiou, C. Diakaki, V. Dinopoulou, A. Kotsialos, and Y. Wang. Review of road traffic control strategies. *Proceedings of the IEEE*, 91(12):2043–2067, 2003.
- [106] M. Papageorgiou and A. Kotsialos. Freeway ramp metering: An overview. *IEEE transactions on intelligent transportation systems*, 3(4):271–281, 2002.
- [107] H. Payne. Models of freeway traffic and control. *Simulation Council Proceedings*, 1:51–61, 1971.
- [108] L. A. Pipes. An operational analysis of traffic dynamics. *Journal of applied physics*, 24(3):274–281, 1953.
- [109] L. A. Pipes. An operational analysis of traffic dynamics. *Journal of Applied Physics*, 24:274–281, 1953.
- [110] J. Ploeg, B. T. Scheepers, E. Van Nunen, N. Van de Wouw, and H. Nijmeijer. Design and experimental evaluation of cooperative adaptive cruise control. In *Proceedings of the 2011 14th International IEEE Conference on Intelligent Transportation Systems (ITSC)*, pages 260–265. IEEE, 2011.
- [111] N. Polson and V. Sokolov. Bayesian analysis of traffic flow on interstate I-55: The LWR model. *arXiv preprint arXiv:1409.6034*, 2014.

- [112] R. Rajamani, S. B. Choi, B. K. Law, J. K. Hedrick, R. Prohaska, and P. Kretz. Design and experimental implementation of control for a platoon of automated vehicles. *AMSE Journal of Dynamic Systems, Measurement, and Control*, 122(3):470–476, 1998.
- [113] A. Reuschel. Vehicle movements in a platoon. *Oesterreichisches Ingenieur-Archiv*, 4:193–215, 1950.
- [114] A. Reuschel. Vehicle movements in a platoon with uniform acceleration or deceleration of the lead vehicle. *Zeitschrift des Oesterreichischen Ingenieur-und Architekten-Vereines*, 95:50–62, 1950.
- [115] P. I. Richards. Shock waves on the highway. *Operations Research*, 4(1):42–51, 1956.
- [116] C. Roncoli, N. Bekiaris-Liberis, and M. Papageorgiou. Highway traffic state estimation using speed measurements: Case studies on NGSIM data and Highway A20 in the Netherlands. In *in Proceedings of the Transportation Research Board 95th Annual Meeting*, number 16-2071, 2016.
- [117] J. Sau, N. El Faouzi, A. B. Assa, and O. De Mouzon. Particle filter-based real-time estimation and prediction of traffic conditions. *Applied Stochastic Models and Data Analysis*, 12, 2007.
- [118] A. Schadschneider and M. Schreckenberg. Cellular automation models and traffic flow. *Journal of Physics A: Mathematical and General*, 26(15), 1993.
- [119] P. Seiler, A. Pant, and K. Hedrick. Disturbance propagation in vehicle strings. *IEEE Transactions on automatic control*, 49(10):1835–1842, 2004.
- [120] T. Seo, A. M. Bayen, T. Kusakabe, and Y. Asakura. Traffic state estimation on highway: A comprehensive survey. *Annual Reviews in Control*, 43:128 – 151, 2017.
- [121] S. E. Shladover. Review of the state of development of advanced vehicle control systems (avcs). *Vehicle System Dynamics*, 24(6-7):551–595, 1995.
- [122] S. E. Shladover, C. A. Desoer, J. K. Hedrick, M. Tomizuka, J. Walrand, W.-B. Zhang, D. H. McMahon, H. Peng, S. Sheikholeslam, and N. McKeown. Automated vehicle control developments in the PATH program. *IEEE Transactions on vehicular technology*, 40(1):114–130, 1991.
- [123] S. E. Shladover, D. Su, and X.-Y. Lu. Impacts of cooperative adaptive cruise control on freeway traffic flow. *Transportation Research Record*, 2324(1):63–70, 2012.
- [124] S. Singh, M. Chen, S. L. Herbert, C. J. Tomlin, and M. Pavone. Robust tracking with model mismatch for fast and safe planning: an sos optimization approach. *arXiv preprint arXiv:1808.00649*, 2018.
- [125] R. E. Stern, S. Cui, M. L. Delle Monache, R. Bhadani, M. Bunting, M. Churchill, N. Hamilton, H. Pohlmann, F. Wu, B. Piccoli, et al. Dissipation of stop-and-go waves via control of autonomous vehicles: Field experiments. *Transportation Research Part C: Emerging Technologies*, 89:205–221, 2018.
- [126] R. E. Stern, S. Cui, M. L. Delle Monache, R. Bhadani, M. Bunting, M. Churchill, N. Hamilton, R. Haulcy, H. Pohlmann, F. Wu, B. Piccoli, B. Seibold, J. Sprinkle, and D. B. Work. Dissipation of stop-and-go waves via control of autonomous vehicles: Field experiments. *Transportation Research Part C: Emerging Technologies*, 89:205 – 221, 2018.
- [127] Y. Sugiyama, M. Fukui, M. Kikuchi, K. Hasebe, A. Nakayama, K. Nishinari, S. i. Tadaki, and S. Yukawa. Traffic jams without bottlenecks – experimental evidence for the physical mechanism of the formation of a jam. *New Journal of Physics*, 10(3):033001, 2008.
- [128] X. Sun, L. Munoz, and R. Horowitz. Highway traffic state estimation using improved mixture Kalman filters for effective ramp metering control. In *42nd IEEE International Conference on Decision and Control (IEEE Cat. No.03CH37475)*, volume 6, pages 6333–6338 Vol.6, Dec 2003.
- [129] X. Sun, L. Muñoz, and R. Horowitz. Mixture Kalman filter based highway congestion mode and vehicle density estimator and its application. In *Proceedings of the American Control Conference*, volume 3, pages 2098–2103, 2004.
- [130] Y. Sun and D. Work. A distributed local kalman consensus filter for traffic estimation. In *Proceedings of the IEEE Conference on Decision and Control*, pages 6484–6491, 2014.

- [131] Y. Sun and D. B. Work. Error bounds for Kalman filters on traffic networks. *Networks & Heterogeneous Media*, 13(2):261–295, 2018.
- [132] Y. Sun and D. B. Work. Scaling the kalman filter for large-scale traffic estimation. *IEEE Transactions on Control of Network Systems*, 5(3):968–980, 2018.
- [133] D. Swaroop and J. Hedrick. String stability of interconnected systems. *IEEE Transactions on Automatic Control*, 41(3):349–357, 1996.
- [134] M. Szeto and D. Gazis. Application of kalman filtering to the surveillance and control of traffic systems. *Transportation Science*, 6(4):419–439, 1972.
- [135] A. Talebpour and H. S. Mahmassani. Influence of autonomous and connected vehicles on stability of traffic flow. In *Transportation Research Board 94th Annual Meeting*, number 15-5971, 2015.
- [136] A. Talebpour and H. S. Mahmassani. Influence of connected and autonomous vehicles on traffic flow stability and throughput. *Transportation Research Part C: Emerging Technologies*, 71:143–163, 2016.
- [137] B. Van Arem, C. J. Van Driel, and R. Visser. The impact of cooperative adaptive cruise control on traffic-flow characteristics. *IEEE Transactions on Intelligent Transportation Systems*, 7(4):429–436, 2006.
- [138] S. Vaskov, S. Kousik, H. Larson, F. Bu, J. Ward, S. Worrall, M. Johnson-Roberson, and R. Vasudevan. Towards provably not-at-fault control of autonomous robots in arbitrary dynamic environments. In *Robotics: Science and Systems*, 2019.
- [139] S. Vaskov, U. Sharma, S. Kousik, M. Johnson-Roberson, and R. Vasudevan. Guaranteed safe reachability-based trajectory design for a high-fidelity model of an autonomous passenger vehicle. In *American Conference on Control*, 2019.
- [140] C. Vivas, S. Siri, A. Ferrara, S. Sacone, G. Cavanna, and F. R. Rubio. Distributed consensus-based switched observers for freeway traffic density estimation. In *Decision and Control (CDC), 2015 IEEE 54th Annual Conference on*, pages 3445–3450. IEEE, 2015.
- [141] R. Wang, S. Fan, and D. B. Work. Efficient multiple model particle filtering for joint traffic state estimation and incident detection. *Transportation Research Part C: Emerging Technologies*, 71:521–537, 2016.
- [142] R. Wang, Y. Li, and D. B. Work. Comparing traffic state estimators for mixed human and automated traffic flows. *Transportation Research Part C: Emerging Technologies*, 78:95–110, 2017.
- [143] R. Wang, D. B. Work, and R. Sowers. Multiple model particle filter for traffic estimation and incident detection. *IEEE Transactions on Intelligent Transportation Systems*, PP(99):1–10, 2016.
- [144] Y. Wang and M. Papageorgiou. Real-time freeway traffic state estimation based on extended Kalman filter: a general approach. *Transportation Research Part B: Methodological*, 39(2):141–167, 2005.
- [145] Y. Wang, M. Papageorgiou, A. Messmer, P. Coppola, A. Tzimitsi, and A. Nuzzolo. An adaptive freeway traffic state estimator. *Automatica*, 45(1):10–24, 2009.
- [146] D. Work, O.-P. Tossavainen, S. Blandin, A. Bayen, T. Iwuchukwu, and K. Tracton. An ensemble Kalman filtering approach to highway traffic estimation using GPS enabled mobile devices. In *Proc. of the 47th IEEE Conference on Decision and Control*, pages 2141–2147, Cancun, Mexico, December 2008.
- [147] D. Work, S. Blandin, O. P. Tossavainen, B. Piccoli, and A. M. Bayen. A traffic model for velocity data assimilation. *Applied Mathematics Research eXpress*, 2010(1):1–35, 2010.
- [148] D. B. Work, S. Blandin, O.-P. Tossavainen, B. Piccoli, and A. Bayen. A traffic model for velocity data assimilation. *Applied Mathematics Research eXpress*, 2010(1):1–35, 2010.
- [149] L. Xiao and F. Gao. A comprehensive review of the development of adaptive cruise control systems. *Vehicle System Dynamics*, 48(10):1167–1192, 2010.

- [150] X. Xu, J. W. Grizzle, P. Tabuada, and A. D. Ames. Correctness guarantees for the composition of lane keeping and adaptive cruise control. *IEEE Transactions on Automation Science and Engineering*, 15(3):1216–1229, 2018.
- [151] Y. Yuan, J. Van Lint, R. E. Wilson, F. van Wageningen-Kessels, and S. P. Hoogendoorn. Real-time lagrangian traffic state estimator for freeways. *IEEE Transactions on Intelligent Transportation Systems*, 13(1):59–70, 2012.
- [152] M. H. Zhang and W. Jin. Kinematic wave traffic flow model for mixed traffic. *Transportation Research Record*, 1802(1):197–204, 2002.